OXFORD

Representing linguistic communicative functions in the premotor cortex

Wenshuo Chang [ID][1,2], Lihui Wang [ID][3,4,5,*], Ruolin Yang [ID][2,6,7,8], Xingchao Wang[9,10,*], Zhixian Gao[9,10], Xiaolin Zhou [ID][1,2,8,11,*]

[1]Institute of Linguistics, Shanghai International Studies University, 1550 Wenxiang Road, Shanghai 201620, China,
[2]Beijing Key Laboratory of Behavior and Mental Health, School of Psychological and Cognitive Sciences, Peking University, 5 Yiheyuan Road, Beijing 100871, China,
[3]Institute of Psychology and Behavioral Science, Shanghai Jiao Tong University, 1954 Huashan Road, Shanghai 200030, China,
[4]Shanghai Key Laboratory of Psychotic Disorders, Shanghai Mental Health Center, Shanghai Jiao Tong University School of Medicine, 600 Wan Ping Nan Road, Shanghai 200030, China,
[5]Shanghai Center for Brain Science and Brain-Inspired Intelligence Technology, 555 Qiangye Road Shanghai 200125, China,
[6]Beijing Neurosurgical Institute, Capital Medical University, 119 South Fourth Ring West Road, Beijing 100070, China,
[7]Peking-Tsinghua Center for Life Sciences, Peking University, 5 Yiheyuan Road, Beijing 100871, China,
[8]IDG/McGovern Institute for Brain Research, Peking University, 5 Yiheyuan Road, Beijing 100871, China,
[9]Department of Neurosurgery, Beijing Tiantan Hospital, Capital Medical University, 119 South Fourth Ring West Road, Beijing 100070, China,
[10]China National Clinical Research Center for Neurological Diseases, 119 South Fourth Ring West Road, Beijing 100070, China,
[11]Shanghai Key Laboratory of Mental Health and Psychological Crisis Intervention, School of Psychology and Cognitive Science, East China Normal University, 3663 North Zhongshan Road, Shanghai 200062, China

*Corresponding authors: Institute of Linguistics, Shanghai International Studies University, Shanghai, China. Email: xz104@pku.edu.cn; Department of Neurosurgery, Beijing Tiantan Hospital, Capital Medical University, Beijing, China. Email: wangxc@mail.ccmu.edu.cn; Institute of Psychology and Behavioral Science, Shanghai Jiao Tong University, Shanghai, China. Email: lihui.wang@sjtu.edu.cn

Linguistic communication is often regarded as an action that serves a function to convey the speaker's goal to the addressee. Here, with an functional magnetic resonance imaging (fMRI) study and a lesion study, we demonstrated that communicative functions are represented in the human premotor cortex. Participants read scripts involving 2 interlocutors. Each script contained a critical sentence said by the speaker with a communicative function of either making a Promise, a Request, or a Reply to the addressee's query. With various preceding contexts, the critical sentences were supposed to induce neural activities associated with communicative functions rather than specific actions literally described by these sentences. The fMRI results showed that the premotor cortex contained more information, as revealed by multivariate analyses, on communicative functions and relevant interlocutors' attitudes than the perisylvian language regions. The lesion study results showed that, relative to healthy controls, the understanding of communicative functions was impaired in patients with lesions in the premotor cortex, whereas no reliable difference was observed between the healthy controls and patients with lesions in other brain regions. These findings convergently suggest the crucial role of the premotor cortex in representing the functions of linguistic communications, supporting that linguistic communication can be seen as an action.

Key words: communication; action; speech act; premotor cortex; mental simulation.

Introduction

Linguistic communication usually engages 2 interlocutors, a speaker and an addressee (Russell 1950; Brennan et al. 2010; Tylén et al. 2010). Linguistic theories, such as Sprachspiel (Wittgenstein 1953) and speech acts theory (Searle 1969; Austin 1975; Searle 1985), propose that language use is a communicative action that serves the function of achieving the speaker's goal, by expressing what is intended to be conveyed to the addressee. The communicative function abstracts from the literal meaning (propositional content) of the speaker's sentence. For example, by saying "Can you reach the salt?" at a dinner table, the speaker intends to request the addressee to pass the salt rather than simply asking about the addressee's ability to reach it. This theoretical insight leads to a notion that considers linguistic communications as goal-directed actions. Understanding the communicative function (e.g. the request) is an essential step for successfully interpreting the speaker's particular goal (e.g. getting the salt) for the addressee who seeks to respond accordingly (Levinson 2016).

Depending on the communicative functions (Searle 1969, 1985), linguistic communications can be categorized into commissives,

directives, and assertives. (Searle has distinguished 5 categories of linguistic communications, commissives, directives, assertives, expressives, and declarations. The present study focused on the first 3 categories.) By commissives, such as to promise or to assure, the speaker shows his/her commitment to conduct a task. By directives, such as to request or to order, the speaker obliges the addressee to conduct a task. While both commissives and directives involve the interlocutors' intention regarding conducts of tasks, assertives, such as replying to a query or stating a fact, involve the description of the situations that can be irrelevant to the interlocutors' intentions. These categories can be differentiated by the interlocutors' attitudes toward the tasks, such as their willingness and their evaluations of the cost–benefit of accomplishing the task (Searle and Vanderveken 1985; Pérez 2001). For example, by saying "I will write a recommendation letter for you" as a promise, the speaker conveys a goal that can benefit the addressee, so that the addressee would have the willingness to have the task accomplished by the speaker. By saying "please write a recommendation letter for me" as a request, the speaker conveys a goal that can benefit the speaker, so that the speaker would have the willingness to have the task accomplished. By saying "I wrote a

recommendation letter for my student" as a reply to the question "What did you do this morning?", the speaker simply describes the situation, and hence the attitude of the interlocutors toward the task in the reply is not clear.

While linguistic communications are regarded as goal-directed actions with different functions by linguistic theories, it is barely known how these communicative functions are represented in the brain. One straightforward prediction is that communicative functions are represented in brain areas that subserve action programing or preparation. Consistent with this prediction, the co-evolution of humans' linguistic ability and motor skills (e.g. tool use) has been highlighted from neurophysiological, neurocognitive, and anthropological perspectives (Rizzolatti and Arbib 1998; Arbib 2011; Stout and Chaminade 2012; Pulvermüller 2018; Thibault et al. 2021). As a demonstration, linguistic communications between tutors and learners can improve the efficiency of learning to make Paleolithic tools (Morgan et al. 2015), and the activation in the premotor region of the human brain increases with the evolutionary progress of Paleolithic tool-making skills (Stout et al. 2008). Moreover, contributions of the premotor region to communications through language or language-like manners are revealed not only in humans (Hauk et al. 2004; Wilson et al. 2004; Egorova et al. 2016; Dreyer and Pulvermüller 2018), but also in species including avian (Thompson et al. 2011), Cercopithecinae (Gil-da-Costa et al. 2006), and *Pan troglodytes* (Bianchi et al. 2016).

For humans, the premotor cortex, consisting of the lateral premotor cortex (LPMC) and medial premotor cortex (MPMC) (Mayka et al. 2006), are broadly involved in action-related processes, such as action execution (Aziz-Zadeh et al. 2006), planning (Gallivan et al. 2013), observation (Aziz-Zadeh et al. 2006), imitation (Aziz-Zadeh et al. 2006), and imagery (Pilgramm et al. 2016). Importantly, the premotor cortex is also found to play a crucial role in human language processing (Gallese and Lakoff 2005; Pulvermüller 2005; Gallese 2008; Pulvermüller and Fadiga 2010; Arbib 2011, 2016; Hertrich et al. 2016; Pulvermüller 2018). The premotor cortex is involved in speech production and perception that engage explicit motor programing of articulator organs (Wilson et al. 2004), and is also involved in language comprehension without such explicit programing (Hauk et al. 2004; Postle et al. 2008; van Ackeren et al. 2012; Feng et al. 2017, 2021). For example, the comprehension of written action verbs involves the activation of the premotor cortex (Hauk et al. 2004), and the processing of action semantics is interfered by transcranial magnetic stimulation (TMS) over the premotor cortex (Willems et al. 2011; Courson et al. 2017).

Moreover, the premotor cortex is not only involved in the language processing that is directly related to action semantics, but also involved in linguistic communications that are not literally related to actions (Shibata et al. 2011; van Ackeren et al. 2012; Feng et al. 2021). Relative to hearing statements about objective situations (e.g. "It is hot here" with a picture of a desert), hearing indirect requests (e.g. "It is hot here" with a picture of a closed window) elicits greater activations in the left LPMC and left MPMC (van Ackeren et al. 2012). Similarly, the indirect reply (e.g. saying "It's hard to give a good presentation") to the addressee's question (e.g. "What did you think of my presentation?") elicits increased activation in the medial frontal cortex extending to the MPMC as compared with a literal reply (Shibata et al. 2011; Feng et al. 2021). Relative to hearing prosodies conveying unambiguous communicative functions, hearing prosodies conveying ambiguous functions engenders stronger activation in the MPMC (Hellbernd and Sammler 2018). Moreover, the premotor cortex is responsive not only to the ambiguity of the communicative functions but

also to the types of communicative functions (Egorova et al. 2016). Relative to a verbal assertive, a verbal request elicits increased activations in the bilateral premotor cortex as well as in the left inferior frontal gyrus and temporal regions.

While some authors explained the involvements of the motor system as reflecting the predictions of particular actions related to communicative functions (e.g. delivering the requested object, Boux et al. 2021; Tomasello et al. 2022), it is less clear if the premotor cortex represents the abstract communicative functions that cover various forms of specific actions. Moreover, given the usual concurrent involvement of the premotor cortex and the left lateralized perisylvian language regions (Shibata et al. 2011; Egorova et al. 2016; Feng et al. 2017, 2021), the latter of which are broadly involved in the processing of semantic and syntactic information (Friederici 2011; Friederici et al. 2017; Hagoort 2017), it is unknown if the premotor cortex functions more or less profoundly in representing communicative functions than the perisylvian regions. The present study aims to test the extent to which the premotor cortex plays a critical role in representing different communicative functions when linguistic communications are understood. To this end, we created scripts of linguistic communications containing critical sentences serving communicative functions while controlling for the semantic content of the critical sentences across these functions, yielding 4 conditions (communicative functions): *Promise* and its control *Reply-1*, as well as *Request* and its control *Reply-2*. We first conducted an functional magnetic resonance imaging (fMRI) study in which participants were instructed to read the scripts. We expected that the different communicative functions conveyed in the scripts can be decoded by the multivariate brain activation patterns. Considering the role of the premotor cortex in representing action-related information, we predicted further that the decoding of communicative functions is more pronounced in the premotor cortex than in the perisylvian regions. Moreover, we predicted that the representation of communicative functions in the premotor cortex is correlated with the interlocutors' attitudes, which are closely related to communicative functions. We also conducted a lesion study on patients with brain lesions to assess the causal role of the premotor cortex in representing communicative functions. We predicted that the understanding of communicative functions would be impaired in the patient group with lesions in the premotor cortex, relative to the patient group with lesions in other brain areas and to the healthy control group.

Materials and methods
Study 1: fMRI study
Participants

Fifty-eight native Chinese speakers (30 females, mean age = 22 years, standard deviation = 3, range: [18, 31]) with normal or corrected-to-normal vision participated in the fMRI experiment. None of them reported a history of neurological or psychiatric disorders. Written informed consent was obtained from each participant prior to the experiment. Two participants were excluded from data analysis due to dropping out. This study was performed in accordance with the Declaration of Helsinki and was approved by the Committee for Protecting Human and Animal Subjects of the School of Psychological and Cognitive Sciences at Peking University.

Design and materials

We created Chinese scripts, each of which consisted of a context, a pre-critical sentence, and a critical sentence. Depending on

Table 1. English translation of the scripts in the fMRI study, with original Chinese version of critical sentences.

Communicative function	Context	Pre-critical sentence	Critical sentence
Promise	The sales department conducted a survey, and Xiaoli was assigned to analyze the survey data this week. But Xiaoli was too busy to analyze it because he had the other assignment recently. His colleague Xiaowu had more spare time this week. And they were communicating with each other.	Then Xiaowu said to Xiaoli:	"I will analyze the survey data this week." "这周我负责分析问卷数据。"
Reply-1	The sales department conducted a survey, and Xiaowu was assigned to analyze the survey data this week. His colleague Xiaoli was assigned to record a working memo, Xiaoli wanted to know about Xiaowu's job assignment. And they were communicating with each other.	Then Xiaowu said to Xiaoli:	"I will analyze the survey data this week." "这周我负责分析问卷数据。"
Request	The sales department conducted a survey, and Xiaowu was assigned to analyze the survey data this week. But Xiaowu was too busy to analyze it because he had the other assignment recently. His colleague Xiaoli had more spare time this week. And they were communicating with each other.	Then Xiaowu said to Xiaoli:	"You will analyze the survey data this week." "这周你负责分析问卷数据。"
Reply-2	The sales department conducted a survey, and Xiaoli was assigned to analyze the survey data this week. His colleague Xiaowu was assigned to record a working memo. Then, Xiaoli wanted to confirm his own job assignment. They were communicating with each other.	Then Xiaowu said to Xiaoli:	"You will analyze the survey data this week." "这周你负责分析问卷数据。"

the contexts, the critical sentences served different communicative functions, yielding 4 conditions: *Promise*, *Reply-1*, *Request*, and *Reply-2*.

Eighty quadruplets of Chinese scripts describing daily-life scenarios were created and selected (Table 1). Each quadruplet included 4 scripts. Each script started with the context of a communication involving 2 interlocutors, a speaker and an addressee. Then a sentence "and they were communicating with each other" was included to introduce the pre-critical sentence "then A (i.e., the speaker) said to B (i.e., the addressee)" and the final critical sentence. The critical sentence was said by the speaker to convey a communicative function.

Each of the 4 scripts in a quadruplet corresponded to 1 of 4 experimental conditions. A specific experimental condition was defined by the communicative function of the critical sentence. Specifically, in the condition termed *Promise*, the context described a task that the addressee was supposed to do but was yet unable to complete for a particular reason and the speaker was capable of doing this task for the addressee. In the following conversation, the speaker said the critical sentence with the first-person subject "I" to express the intention to do the task. In the condition termed *Reply-1*, the context described the same task as the task in the *Promise* condition but specified that it was the speaker who was supposed to complete the task. In the following conversation, the speaker said the critical sentence with the first-person subject to state that the speaker would do the task. The *Reply-1* condition served as the control condition for the *Promise* condition in the way that the critical sentences in the 2 conditions were the same, but these 2 critical sentences served different communicative functions. In the condition termed *Request*, the context described the same task as above that the speaker was supposed to do yet was unable to complete for a particular reason, and the addressee was capable of doing this task for the speaker. In the following conversation, the speaker said the critical sentence with the second-person subject "*You*" to express the intention to request the addressee to do the task. In the condition termed

Reply-2, the context described the same task that the addressee was supposed to complete. In the following conversation, the speaker said the critical sentence with the second-person subject to describe that the addressee would do the task. The *Reply-2* condition served as the control condition for the *Request* condition in the way that the critical sentences in the 2 conditions were the same, but these 2 critical sentences served different functions. The pre-critical sentence was consistent across the 4 conditions in a quadruplet because the identities of the speaker and the addressee were invariable. The critical sentences varied only in the subjects and described the conduct of the same task across 4 conditions, resulting in identical critical sentences for *Promise* and *Reply-1* and for *Request* and *Reply-2*, respectively.

These scripts were selected based on the evaluative results from an independent group of participants in a pilot evaluation prior to the fMRI experiment (see *Results* for the summary of the pilot results and Supplemental Information for details).

The 80 quadruplets of scripts (320 scripts in total) were assigned into 4 experimental lists according to a Latin-square procedure. Each experimental list included 80 scripts, with 20 scripts for each condition. In a specific experimental list, 80 scripts came from the 80 different quadruplets such that there was no repetition of a specific critical sentence. For each participant, based on the Latin-square design, scripts from one of the experimental lists were used as the reading materials. The 80 scripts (trials) were divided into 5 scanning runs (16 scripts per run), each of which lasted approximately 7 min. Trials of the 4 conditions were equally distributed in the 5 scanning runs. In each run, trials of different conditions were mixed and presented in a pseudo-randomized order with the restriction that no more than 3 scripts with the same communicative function were presented consecutively.

Experimental presentation was programmed using MATLAB Psychtoolbox (Brainard 1997; Pelli 1997). Each participant was asked to silently read a list of scripts in the magnetic resonance (MR) scanner. Stimuli were presented in black (RGB: 0, 0, 0) against
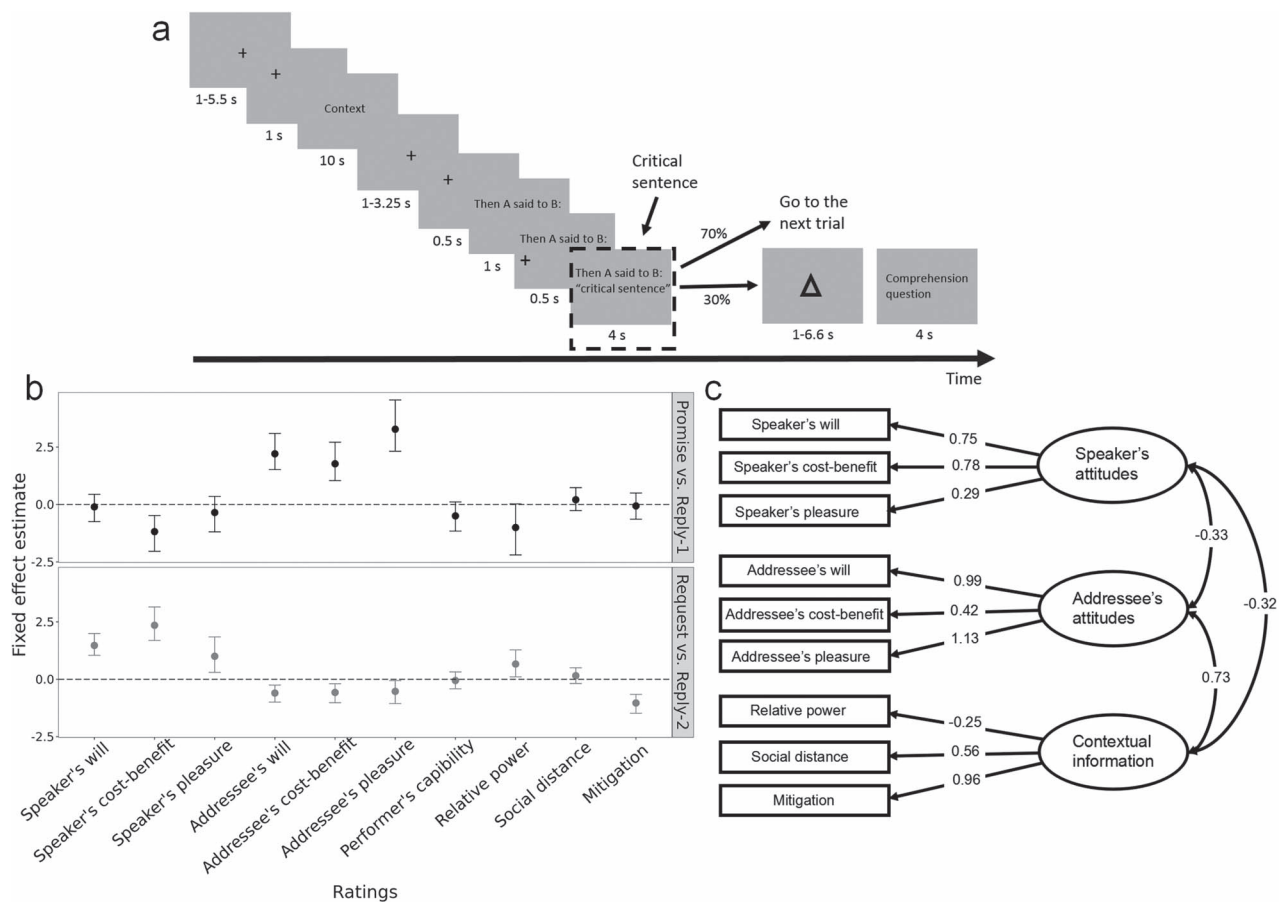
Fig. 1. Experimental procedure and behavioral results of the fMRI study. a) In each trial, the context, the pre-critical sentence, and the critical sentence were presented sequentially in written form. The critical sentence is enclosed by the dashed rectangle (not shown in the actual experiment). In 24 catch trials (30% of all trials), participants were instructed to respond to a comprehension question. b) Results of Bayesian logistic mixed modeling. The posterior estimates of the fixed effects (vertical axis) for rating features (horizontal axis) in the "*Promise vs. Reply-1*" model (upper panel, black) and the "*Request vs. Reply-2*" model (lower panel, gray) are illustrated. The solid dots represent mean posterior estimates, the error bars represent 95% CrIs. A 95% CrI excluding 0 indicates a statistically significant predictability of the corresponding feature. c) The 3-factor model of the CFA. The ellipses represent the accounting factors and the rectangles represent the rating features. The correlations between the accounting factors and the loadings of the accounting factors on the features are embedded in the arrows.

a gray background (RGB: 180, 180, 180). In each trial (Fig. 1a), a fixation cross was firstly presented at the center of the screen for a jitter duration of 1–5.5 s, followed by a cross presented at the upper left part of the screen where the first character of the context would located. This fixation was presented for 1 s to direct participants' attention. The context was presented for 10 s and followed by a cross presented at the center for another jitter duration of 1–3.25 s. A cross was then presented for 1 s at the upper left part of the screen where the first character of the pre-critical sentence was located. After the offset of the cross, the pre-critical sentence was presented. After the pre-critical sentence had been presented for 1 s, a cross was presented below the pre-critical sentence, where the first character of the critical sentence would be located. This cross lasted for 0.5 s together with the pre-critical sentence. After the offset of the cross, the critical sentence was presented within double quotes for 4 s, together with the pre-critical sentence. To engage the participants into reading the script, a comprehension question, which was related to the information of both the contexts and the critical sentences, was added to each of the 24 catch trials (30% of all trials, each condition had 6 catch trials). At the end of these catch trials, a triangle was presented at the center for a jitter duration of 1–6.6 s, followed by a comprehension question. Participants were instructed to make "yes" or "no" response by pressing the button on the response box

in their left or right hand. Half of the participants were instructed to press the left button for "yes" and the right button for "no," and the other half made their responses with a reversed button-hand assignment. Half of these trials required a "yes" as correct response and the other half required a "no" as correct response. Prior to the scanning, participants performed 10 practice trials with scripts not in the experimental lists.

Post-scanning ratings for experimental scripts

To quantify interlocutors' attitudes and the contextual information related to communicative functions, participants were asked to fulfill a post-scanning rating task on the same scripts they read in the MR scanner after the scanning. They were asked to rate each of the 10 features for each script. These 10 features were the same as those rated in the pilot evaluation (see Supplemental Information). A 7-point scale was used for each of these features: (1) performer's capability, from 1 (the performer is not capable of conducting the task described by the critical sentence) to 7 (the performer is very capable of conducting the task); (2) speaker's will and (3) addressee's will, from 1 (the speaker/addressee is very unwilling to conduct the task) to 7 (the speaker/addressee is very willing to conduct the task); (4) speaker's cost–benefit and (5) addressee's cost–benefit, from 1 (the speaker/addressee would pay a high cost if the task has been accomplished) to 7

(the speaker/addressee would be benefitted highly if the task has been accomplished); (6) speaker's pleasure and (7) addressee's pleasure, from 1 (the speaker/addressee is very unpleased when communicating) to 7 (the speaker/addressee is very pleased when communicating); (8) relative power, from 1 (the addressee's power is definitely higher than the speaker's) to 7 (the speaker's power is definitely higher than the addressee's); (9) the social distance between the interlocutors, from 1 (very close) to 7 (very remote); and (10) mitigation of the critical sentence, from 1 (not mitigated at all) to 7 (highly mitigated).

Statistical analysis of post-scanning ratings
Bayesian logistic mixed models
To assess the extent to which communicative functions could be predicted by the 10 features, the post-scanning ratings were fitted with Bayesian logistic mixed models using the *brms* package (Bürkner 2017) in R environment. The 2 pair-wise predictions, "*Promise* vs. *Reply-1*" and "*Request* vs. *Reply-2*", were assessed respectively with an independent model. In each model, the response variable was the communicative function, the predictors were the ratings of the 10 features. Full models were fitted to reduce type-I error rate (Barr et al. 2013). The priors for all fixed slopes and the fixed intercept were *Normal*(0,100), while the priors for standard deviations were *Cauchy*(0,5). Within the variance–covariance matrices of the by-participant and by-item random effects, priors were defined for the correlation matrices using a Lewandowski-Kurowicka-Joe (LKJ) prior with parameter η 1.0 (Lewandowski et al. 2009). The joint posterior distribution was sampled by 4 Monte-Carlo Markov Chains (MCMCs) at 20,000 iterations for each model, with the first half of the samples discarded as warm-up samples. Convergence was checked using $\hat{R}$ convergence diagnosis (Gelman and Rubin 1992). Mean estimates (*b*) and 95% credible intervals (CrIs) of posterior distributions were used to evaluate the fitted coefficients. All posterior estimates reported have $\hat{R}$-values lower than 1.01. The predictability of each rating feature was indexed by the corresponding posterior estimate, and the estimate was considered as statistically significant when the 95% CrI excluded 0.

Factor analyses
To evaluate the reliability of the 3-factor model estimated by the exploratory factor analysis (EFA) (Supplemental Information) on the post-scanning ratings, a confirmatory factor analysis (CFA) with the factor structure obtained by the EFA was conducted using the *lavaan* package (Oberski 2014) in R. The CFA model was evaluated by comparative fit index (CFI), Tucker-Lewis index (TLI), and root mean square error of approximation (RMSEA).

MRI data acquisition and preprocessing
A GE-MR750 3T MR scanner was used to collect T1-weighted structural images with $1 \times 1 \times 1$ mm^3 voxel size and functional images. In each run of fMRI, an echo-planar imaging (EPI) sequence with an interleaved (bottom-up) acquisition order, 2,000 ms repetition time, 30 ms echo time, and 90° flip angle to obtain 225 3D volumes of the whole brain. Each volume consisted of 33 axial slices covering the whole brain. Slice thickness was 3.5 mm and inter-slice gap was 0.7 mm, with a 224 mm field of view (FOV), 64×64 matrix, and $3.5 \times 3.5 \times 4.2$ mm^3 voxel size. Head motion was minimized using cushions around the head and a forehead strap.

The preprocessing of fMRI data was implemented using fMRI Expert Analysis Tool (FEAT) in FSL (FMRIB Software Library v5.0.11) (Jenkinson et al. 2012). To ensure steady state magnetization, the first 5 volumes were discarded. Preprocessing consisted of brain extraction using Brain Extraction Tool (BET) based on the structural image (Smith 2002), motion correction using Motion Correction FMRIB's Linear Image Registration Tool (MCFLIRT) (Jenkinson et al. 2002), slice-timing with Fourier-space time-series phase-shifting, spatial smoothing with a Gaussian kernel of Full-Width Half-Maximum (FWHM) 5 mm, high-pass temporal filtering with a cutoff of 100 s, and grand-mean intensity normalization of the entire 4D dataset by a single multiplicative factor. These preprocessing procedures were applied on fMRI data for both univariate and multivariate analyses, except that spatial smoothing was skipped for the multivariate analyses. To co-register the structural image and the functional images, a linear transformation with 12 degrees of freedom (df) allowing translation and rotation was applied by FLIRT (Jenkinson and Smith 2001; Jenkinson et al. 2002). The 12 df linear transformation from the structural image to the Montreal Neurological Institute (MNI) system was further refined using FNIRT registration with a nonlinear algorithm for 54 participants' images, whereas the registration with linear algorithm was used for the other 2 participants' images for better alignment.

Region of Interest (ROI) definitions
The bilateral premotor cortex, including MPMC and LPMC, were defined based on the probability maps of the Jülich Histological atlas (Geyer 2004). In the premotor cortex (Fig. 2a), voxels with an absolute value of x coordinate in the MNI system lower than 16 were assigned to MPMC, otherwise, they were assigned to LPMC (Mayka et al. 2006).

Four ROIs in the left lateralized perisylvian language region, including the BA44 division of the Broca's area (left BA44), BA45 division of the Broca's area (left BA45) (Amunts et al. 1999), left middle temporal gyrus (LMTG), and left superior temporal gyrus (LSTG) (Desikan et al. 2006) were defined based on the probability maps of the Jülich Histological atlas and the Harvard-Oxford Cortical atlas (Fig. 2a).

For all ROIs, only voxels with a probability greater than 20% were reserved. Each voxel was assigned to a ROI according to its maximum probability among the above mentioned 5 ROI probability maps.

General linear model
For each participant and each run, 4 regressors were respectively defined for the 4 experimental conditions, *Promise*, *Reply-1*, *Request*, and *Reply-2*, by the onsets of the critical sentence with a duration of 4 s convolved by canonical hemodynamic response function (HRF). The temporal derivative of each of the 4 regressors was included as a regressor of no-interest. Another 3 regressors respectively corresponding to the context, the pre-critical sentence, and the comprehension question were also included. The 6 parameters of head movements were added in to reduce the influence of head motion on signal changes.

Univariate analyses
To examine if the univariate activities differed between the conditions, both whole-brain and ROI-based univariate analyses were conducted (see Supplemental Information for detailed methods and results). While the univariate results showed the involvements of the premotor cortex and the perisylvian regions in processing specific communicative functions, they cannot address whether the ROIs showed distinctive activity patterns under different conditions. We thus focused on multivariate activity patterns in the following analysis.
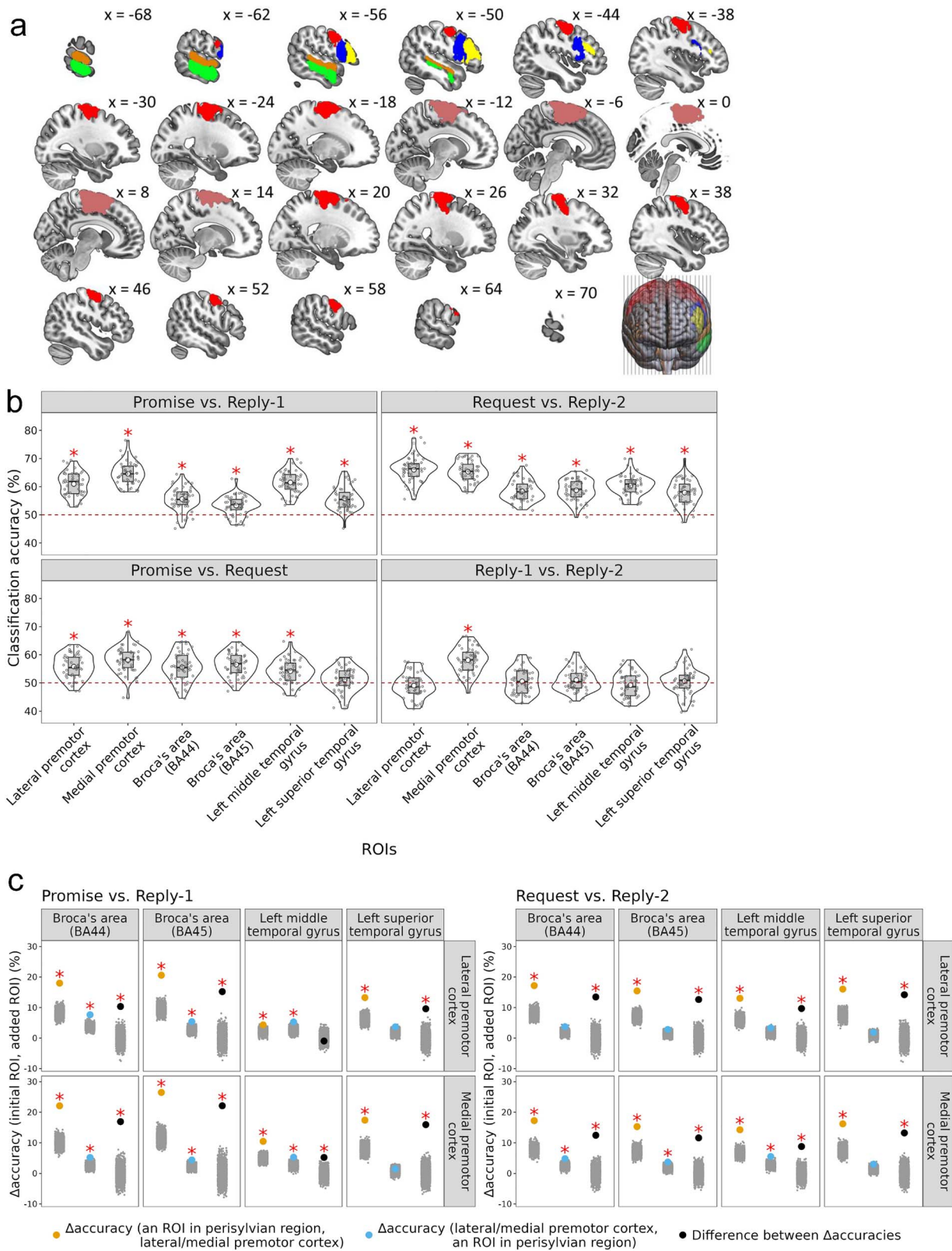
Fig. 2. MVPC results of fMRI data. a) Five ROIs were defined. Red, LPMC; pink, MPMC; blue, Broca's area (BA44); yellow, Broca's area (BA45); green, LMTG; orange, LSTG (*x*-coordinates based on the MNI system). b) Results of ROI-based MVPCs. The classification accuracies (vertical axis) in the ROIs (horizontal axis) for the 4 pair-wise classifications are illustrated. Left top, *Promise* vs. *Reply-1*; right top, *Request* vs. *Reply-2*; left bottom, *Promise* vs. *Request*; right bottom, *Reply-1* vs. *Reply-2*. The red dashed lines represent the chance-level percentage of binary classification (50%). Red stars represent statistical significance of permutation tests with Bonferroni correction. c) Results of combinatorial MVPCs. Left panel, *Promise* vs. *Reply-1*; right panel, *Request* vs. *Reply-2*. Vertical axes illustrate the improvement in classification accuracy contributed by an added ROI for an initial ROI. Red stars represent statistical significance of permutation tests with Bonferroni correction. Each yellow dot indicates the improvement in classification accuracy contributed by a premotor ROI for a perisylvian ROI. Each blue dot indicates the improvement in classification accuracy contributed by a perisylvian ROI for a premotor ROI. Each black dot indicates the difference between the improvement in classification accuracy contributed by a premotor ROI for a perisylvian ROI and that contributed by a perisylvian ROI for a premotor ROI. The crowded small gray dots indicate data points of null distributions for permutation tests.

ROI-based multivariate pattern classification

To detect differences in activity patterns representing the different communicative functions, multivariate pattern classification (MVPC) was conducted for each ROI using the *PyMVPA* toolbox (Hanke et al. 2009). In each ROI, the voxel-level parameter estimates of the critical sentences were extracted, detrended along time series, and transformed into *Z*-scores across runs. For each ROI, cross-validated classifications of communicative functions were performed using a linear support vector machine (SVM) as a classifier. Four pair-wise classifications were performed: (1) *Promise* vs. *Reply-1*; (2) *Request* vs. *Reply-2*; (3) *Promise* vs. *Request*; (4) *Reply-1* vs. *Reply-2*. For each pair-wise classification, a participant-based cross-validation with 50 repetitions were conducted. Each repetition consisted of a training set of data from 45 (approximately 80% of all data) randomly selected participants and a test set of data from the remaining 11 participants (approximately 20% of all data). For each repetition, a cross-validated accuracy was computed as a percentage of correct classifications of the test set to evaluate the performance of a classifier, and the mean accuracy averaged over the 50 repetitions was calculated.

Statistical significance of the classification accuracy was tested using permutation-based classifications with 2,000 repetitions for each pair-wise classification (Stelzer et al. 2013). In each repetition, the participant-based cross-validation procedure described above was performed on the data with permuted communicative functions, generating 2,000 null cross-validated accuracies derived for each pair-wise classification. Probabilities (*P*-values) of the observed accuracies against the distribution of the permutation-based null accuracies were computed. Statistical significance was determined by a Bonferroni-corrected significance threshold of $P < 0.002$ (24 comparisons were conducted in total). A significant accuracy indicates that the multivariate activity in an ROI showed distinct patterns between the pair-wise communicative functions, leading to an inference that the ROI represents the information on these functions, but the accuracy does not indicate whether or not the ROI is activated for a specific communicative function.

Combinatorial MVPC

To examine whether the L/MPMC represented more information on communicative functions relative to the ROIs in the perisylvian region, combinatorial MVPCs (Clithero et al. 2009; Carter et al. 2012) were conducted. The current analyses focus on 2 pair-wise classifications, "*Promise* vs. *Reply-1*" and "*Request* vs. *Reply-2*".

(1) To test whether the premotor ROIs and the perisylvian ROIs improved classification performance to each other, we conducted 32 (2 premotor ROIs × 4 perisylvian ROIs × 2 pairwise classifications × 2 alternatives of initial-added ROIs pair) permutation tests with 2,000 repetitions. For each test, 50 cross-validated accuracies of the initial ROI and 50 cross-validated combinatorial accuracies served as observations. These 2 types of cross-validated accuracies were permuted and used to compute a null Δaccuracy(initial ROI, added ROI) every repetition, generating a set of null Δaccuracy(initial ROI, added ROI), and *P*-value for the observed accuracy against the null distribution was computed. Statistical significance was determined by Bonferroni-corrected significance threshold of $P < 0.0016$.

(2) To test whether the premotor ROIs represented more information on communicative functions relative to the perisylvian ROIs, we conducted 16 (2 premotor ROIs × 4 perisylvian ROIs × 2 pair-wise classifications) pair-wise permutation tests with 2,000 repetitions to compare Δaccuracy(an ROI in the perisylvian region, L/MPMC) with Δaccuracy(L/MPMC, an ROI in the perisylvian region). For each test, the 2 types of Δaccuracies were permuted every repetition to generate a set of null differences between Δaccuracy(an ROI in the perisylvian region, L/MPMC) and Δaccuracy(L/MPMC, an ROI in the perisylvian region), and the *P*-value of the observed difference against the null distribution was computed. Statistical significance was determined by a Bonferroni-corrected significance threshold of $P < 0.003$.

Representational similarity analyses

Representational similarity analyses (RSAs; Kriegeskorte et al. 2008) were conducted to further examine if the 6 ROIs represent the information on the speaker's attitudes and the addressee's attitudes, and if the premotor ROIs represented more information on the speaker/addressee's attitudes relative to the perisylvian ROIs. These analyses were implemented for 2 pair-wise predictions, "*Promise* vs. *Reply-1*" and "*Request* vs. *Reply-2*", respectively.

Six brain representational dissimilarity matrices (RDMs) and 3 behavioral RDMs were created for each pair-wise prediction (Fig. 3a). For each participant, the general linear model (GLM) was refitted with the same definitions of regressors as described above, except that the critical sentence of every trial was defined

$$\Delta \text{accuracy (initial ROI, added ROI)} \% = \frac{\text{Accuracy (combination of initial ROI and added ROI)} - \text{Accuracy (initial ROI)}}{\text{Accuracy (initial ROI)}} \times 100\% \qquad (1)$$

The computation is performed by Eq. (1). Combinatorial accuracy, Accuracy(combination of initial ROI and added ROI), was the cross-validated accuracy based on voxels collapsed over an initial ROI and an added ROI. Δaccuracy(initial ROI, added ROI) was obtained by subtracting the cross-validated accuracy based on the voxels in an initial ROI, i.e. Accuracy(initial ROI), from the combinatorial accuracy, and dividing this difference by the Accuracy(initial ROI).

This Δaccuracy(initial ROI, added ROI) is an index to quantify the extent to which the added ROI improved classification performance based on the initial ROI. These allow us to examine improvements in classification accuracy contributed by a premotor ROI for each of the perisylvian ROIs and vice versa.

Two steps of permutation-based significance testing were conducted on Δaccuracy(initial ROI, added ROI):

as a single regressor. Hence, each GLM had 80 regressors of the critical sentences. For each ROI of each participant, to avoid over-fitting, feature selection was conducted on the voxels of each ROI (Hanke et al. 2009), and voxels with the 50% highest *F* values were included in the RSA. For the selected voxels, parameter estimates of the critical sentences from the GLM were extracted and transformed into *Z*-scores. Pattern similarity matrix of each ROI was built up by calculating the Pearson correlation of the voxel-wise *Z*-scores between each 2 trials. Then the RDM was obtained by 1—similarity matrix, resulting in a 40 (2 conditions × 20 trials per condition) × 40 brain RDM for each ROI of each participant. For each participant, based on the post-scanning ratings and the 3-factor model obtained by the factor analyses, independent behavioral RDMs were built up to represent the variance of the speaker's attitudes (Speaker
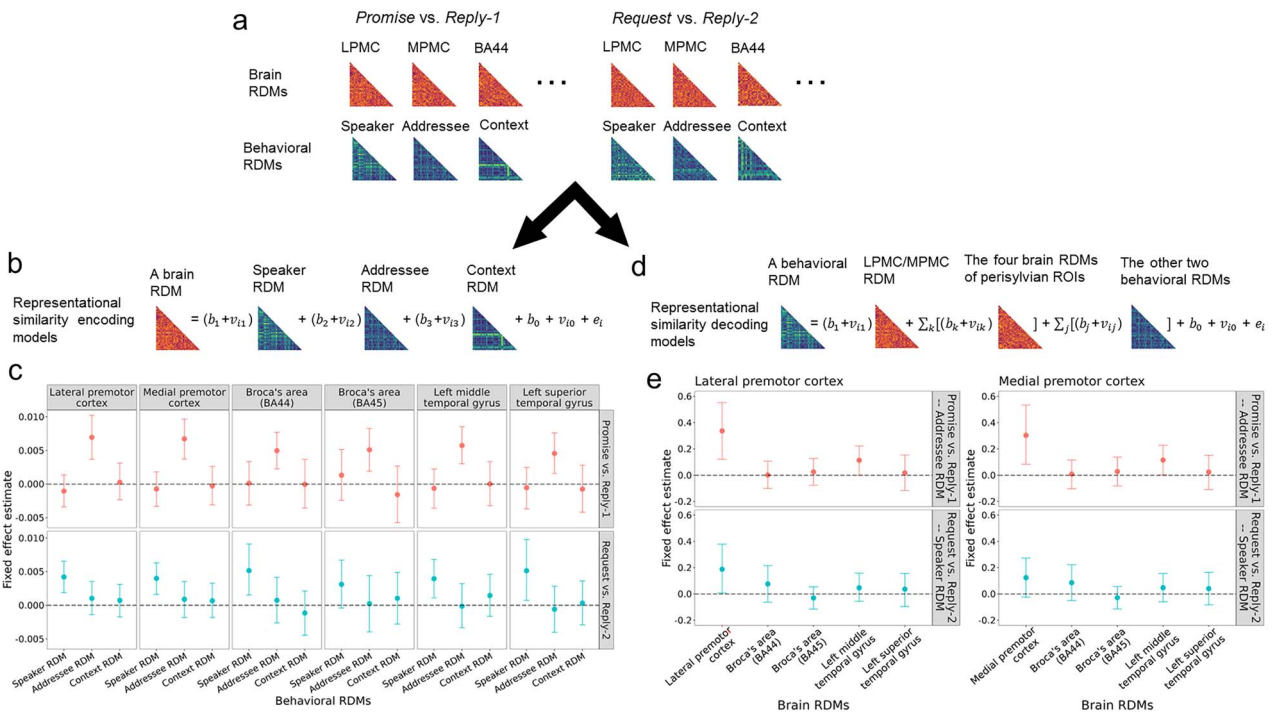
Fig. 3. RSAs of fMRI data. a) The brain RDMs and the behavioral RDMs for the 2 pair-wise predictions, "*Promise* vs. *Reply-1*" and "*Request* vs. *Reply-2*". b) The equation of the RS encoding model, which includes a brain RDM as response variable and the 3 behavioral RDMs as predictors (see Methods for details). c) Results of RS encoding models. d) The equation of the RS decoding model, which includes a behavioral RDM as response variable, 5 brain RDMs as predictors, and the other 2 behavioral RDMs as covariates (see *Methods* for details). e) Left panel, results of RS decoding models with the LPMC RDM and the RDMs of the prerisylvian ROIs as predictors; right panel, results of RS decoding models with the MPMC RDM and the RDMs of the perisylvian ROIs as predictors. For a, b, and d, the lower-triangular RDMs from one participant are shown as examples (only for illustrative purpose). For c and e, the posterior estimates (vertical axis) of the "*Promise* vs. *Reply-1*" models (upper panel, red) and the "*Request* vs. *Reply-2*" models (lower panel, turquoise) are illustrated. The solid dots represent mean posterior estimates, the error bars represent Bonferroni corrected CrIs (99.86% CrI for the encoding models and 99.92% CrI for the decoding models). The dashed gray lines indicate 0 for fixed effect estimates. An effect was determined as significant when the Bonferroni-corrected CrI excluded 0.

RDM), the variance of the addressee's attitudes (Addressee RDM), and the variance of the contextual information (Context RDM), respectively. For each behavioral factor, the ratings of the 3 dimensions for each trial were represented in a 3-dimensional space, and the Euclidian distance between each 2 rating points was calculated as the value in each cell of the behavioral RDM. Each of the 3 behavioral RDM also had a 40 (2 conditions × 20 trials per condition) × 40 structure.

For each ROI and each of the 2 pair-wise predictions, a representational similarity (RS) encoding model was used to assess the extent to which the brain RDM can be predicted by the behavioral RDMs (Fig. 3b). Specifically, a Bayesian linear mixed model was conducted with Eq. (2), where the brain RDM was included as the response variable and the 3 behavioral RDMs as the predictors. In each model, the response variable **Brain_RDM**$_i$ indicates the brain RDM of the ith participant ($i \in [1, 56]$). The predictor $Behavioral\_RDM_{ik}$ indicates one of the behavioral RDMs ($k \in [1, 3]$) of the ith participant. Fixed effects consisted of the fixed slopes b_k and the fixed intercept b_0. Random effects consisted of by-participant random slope v_{ik} for the kth behavioral RDM and random intercept v_{i0} for the ith participant. The model also included the ith participant's residual e_i. Only the lower triangular RDMs were used in these analyses. The model-fitting method was identical to the analysis of the post-scanning ratings. All posterior estimates reported have $\hat{R}$ lower than 1.01.

$$Brain\_RDM_i = \sum_{k=1}^{3}(b_k + v_{ik})Behavioral\_RDM_{ik} + b_0 + v_{i0} + e_i \quad (2)$$

For each of the 2 pair-wise predictions and each of the behavioral RDMs, a RS decoding model was used to assess the extent to which the behavioral RDM can be predicted by the brain RDMs (Fig. 3d). Specifically, a Bayesian linear mixed model was conducted with Eq. (3), where the behavioral RDM was included as the response variable and the RDMs of 5 ROIs as the predictors.

$$Behavioral\_RDM_i = \sum_{k=1}^{5}(b_k + v_{ik})Brain\_RDM_{ik}$$
$$+ \sum_{j=1}^{2}Behavioral\_RDM_{ij} + b_0 + v_{i0} + e_i \quad (3)$$

In each model, the response variable **Behavioral_RDM**$_i$ indicates the behavioral RDM of the ith participant ($i \in [1, 56]$). The predictors $Brain\_RDM_{ik}$ indicate one of the ith participant's 5 brain RDMs ($k \in [1, 5]$), which were RDMs of the 4 perisylvian ROIs and an RDM of one of the premotor ROIs (the RDMs of LPMC and MPMC were included in distinct models respectively to prevent co-linearity). To regress out variances of the ith participant's 2 behavioral RDMs other than the **Behavioral_RDM**$_i$, they were included in the model as covariates $Behavioral\_RDM_{ij}$. The meaning of the remaining parameters in Eq. (3) were the same as the RS encoding model. The model-fitting method was identical to the analyses of the post-scanning ratings. All posterior estimates reported have $\hat{R}$ lower than 1.01.

As described above, while the RS encoding model estimated the coefficients of the different behavioral RDMs in predicting the

brain RDM of a specific ROI, the RS decoding model estimated the coefficients of the brain RDMs of different ROIs in predicting a specific behavioral RDM. An effect was tested with Bonferroni corrected CrIs, 99.86% CrI for the encoding models where 24 (6 brain RDMs × 3 behavioral RDMs × 2 pair-wise predictions) effect estimates were tested, and 99.92% CrI for the decoding models where 60 (3 behavioral RDMs × 5 brain RDMs × 2 models with different premotor ROIs × 2 pair-wise predictions) effect estimates were tested. An effect was determined as significant when Bonferroni corrected CrI excluded 0.

Study 2: lesion study
Participants

Twenty-nine adult patients with unilateral lesions recruited from the Patient's Registry of Beijing Tiantan Hospital (Beijing, China) participated in the experiment. Their lesions resulted from the surgical removal of low-grade gliomas. Depending on the lesion locations, the patients were assigned to either the premotor cortex lesion group or lesion control group. Thirty healthy adults without a known history of psychiatric or neurological disorder were recruited from the local community as a healthy control group. All participants are native Chinese speakers with normal or corrected-to-normal vision and right-handed, with handedness assessed by the Chinese Handedness Questionnaire (Li 1983). Two lesion control participants and 3 healthy control participants were excluded from the data analyses due to poor task performances (see below). This study was performed in accordance with the Declaration of Helsinki and was approved by the Committee for Protecting Human and Animal Subjects of the School of Psychological and Cognitive Sciences at Peking University and the Institutional Review Board of the Beijing Tiantan Hospital at Capital Medical University.

The demographic variables of the participants are shown in Supplemental Table S7. The comparisons of the demographic variables were conducted by independent-sample *t*-tests. The lesion sizes and the chronicities were comparable between the premotor lesion patients and lesion controls (all *P*-values > 0.2). Participants' mental states were assessed with the Mini-Mental State Examination (MMSE, Hamilton et al. 1976) and the Beck depression inventory (BDI, Knight 1984). The MMSE scores and the BDI scores were comparable between all groups (all *P*-values > 0.1). Years of education were comparable between the premotor lesion patients and lesion controls ($P = 0.734$). The years of education of healthy controls were slightly higher than the premotor lesion patients and lesion controls, but this difference did not reach significance ($P = 0.057; P = 0.065$, respectively). While the participants' ages were comparable between the premotor lesion patients and lesion controls and between the premotor lesion patients and healthy controls (*P*-values > 0.1), lesion controls were older than healthy controls on average ($t_{(18.1)} = 2.58$, $P = 0.019$).

Participants' manual dexterities were assessed by the time (in seconds) needed for completing the Grooved Pegboard Test (Lafayette Instrument; https://lafayetteevaluation.com/products/grooved-pegboard), as shown in Supplemental Table S7. The group difference in dexterities was tested using an independent-sample *t*-test. All participants completed the Grooved Pegboard Test with the left and right hands respectively, with the following exceptions: (1) one premotor lesion patient performed the test and the main experimental task with only the left hand because of the hemiparesis caused by the left hemisphere lesion; (2) 2 healthy participants did not perform the test at all. The times for completing the Grooved Pegboard Test with the left hand

were comparable between the premotor lesion patients and the lesion controls, and between lesion controls and healthy controls (all *P*-values > 0.1). The time for premotor lesion patients was numerically longer than that for healthy controls (78 vs. 70 s), but this difference did not reach significance ($P = 0.062$). The times for completing with the right hand were comparable between the premotor lesion patients and healthy controls, and between lesion controls and healthy controls (all *P*-values > 0.1). The time for premotor lesion patients was numerically longer than that for lesion controls (73 vs. 66 s), but this difference did not reach significance ($P = 0.065$). These results indicated that all patients' manual dexterities were qualified for performing the main experimental task.

Lesion reconstruction and group assignment for patients

Two neurosurgeons (the third author and the forth author) identified the lesions of each patient and created the lesion masks based on the structural images. The lesion masks were transformed into the MNI system by linear registration using FSL. For each patient, there were 4 steps of the registration. First, based on T1-weighted structural image, a white matter mask was extracted using the *fast* function (Zhang et al. 2001). Second, based on the T1-weighted image, the white matter mask, and the lesion mask, the lesion area in the T1-weighted image was filled using the *lesion_filling* function (Battaglini et al. 2012). Third, the filled T1-weighted image was transformed into the MNI system by linear registration. This registration generated a transformed matrix of the spatial relation between the filled T1-weighted image and the MNI system. Finally, based on the transformed matrix, the lesion mask was transformed into the MNI system. To ensure the results of the registrations were consistent with the patients' clinical situation, the neurosurgeons further checked and modified the transformed lesion masks. We computed the overlapped volume between each transformed lesion mask and the premotor cortex probability maps of the Jülich Histological atlas. Fourteen patients with overlapped volumes larger than 2 mL were assigned to the premotor lesion group (Fig. 4a), 15 other patients were assigned to the lesion control group (Fig. 4b). In the lesion control group, 4 patients had lesions in the left frontal cortex, four in the right frontal cortex, 4 in the left insula, one in the right temporal cortex, one in the right occipital cortex, and one in the right parietal cortex. See Supplemental Table S8 for detailed information on the patients' lesion regions.

Design and procedure

Eighty-four quadruplets of scripts were created. The structure of the scripts and the experimental design were the same as the fMRI study with the exception that the contents of the scripts were easier to understand to accommodate the patients' cognitive states. To evaluate the reliability of the scripts, 2 pilot studies with independent groups of participants were conducted beforehand (Supplemental Information). We firstly evaluated the scripts and replicated the pattern of results in the fMRI post-scanning ratings, and secondly assessed the appropriateness of the experimental procedure (see below). The results indicated that healthy adults were able to understand the scripts and to complete the task following instructions (Supplemental Information).

The scripts were assigned into 4 experimental lists according to a Latin-square procedure. Each list included 84 scripts (trials), and each list was further divided into 4 sections corresponding to 4 experimental blocks. Each participant was presented a list of scripts with a pseudo-randomized order. No more than 3
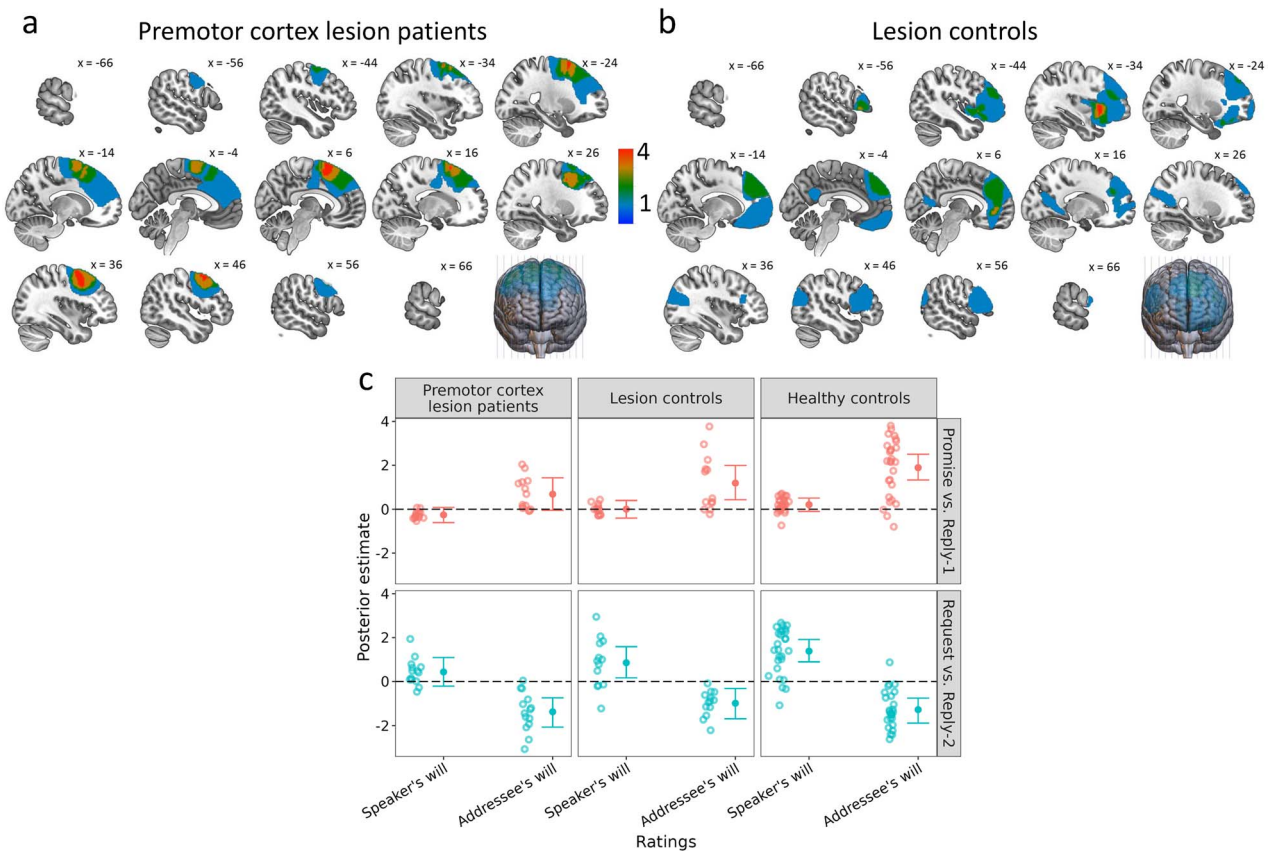
Fig. 4. Results of the lesion study. Lesion reconstructions for a) premotor cortex lesion patients and b) lesion controls. The text in black indicates the *x* coordinates in the MNI system. The color bar indicates the number of patients. c) Results of the Bayesian hierarchical logistic model in the lesion study. The posterior estimates of the ratings (vertical axis) of the speaker's will and addressee's will (horizontal axis) for the premotor lesion patients (left), lesion controls (middle), and healthy controls (right) are plotted. The upper panel represents the "*Promise* vs. *Reply-1*" model, the lower panel represents the "*Request* vs. *Reply-2*" model. The solid circles represent mean group-level posterior estimates. The error bars represent 95% CrIs. A 95% CrI excluding 0 indicates a significant group-level effect. The hollow circles on the left side of the group-level estimates represent the corresponding mean participant-level estimates for all the participants.

scripts with the same communicative function were presented consecutively.

Experimental presentation was programmed using MATLAB Psychtoolbox (Brainard 1997; Pelli 1997). The experiment began with 10 practice trials, followed by the 4 blocks of the main experiment. Each block began with a warm-up trial. The scripts used for the practice trials and the warm-up trials were not in the experimental lists. Each trial of the main experiment had the same sequence of the events of the script presentations as the fMRI experiment, except that the duration of each event was longer to accommodate the patients' cognitive state (Supplemental Fig. S1). After the presentation of the critical sentence, participants were instructed to respond to 3 or 4 questions. First, they were instructed to judge who would perform the action described in the critical sentence (i.e. the performer judgment) within 10 s. The names of the speaker and the addressee were randomly presented on the left bottom and the right bottom of the screen respectively, participants had to choose either of the names by pressing the button on the corresponding side. Second, they were instructed to rate the speaker's will and the addressee's will on a 7-point scale, each of which had to be completed within 20 s. To accommodate the patients' cognitive state, the whole script was presented at the top of the screen to allow them to reread the script. The 2 ratings were presented in random order. To engage participants into the reading, 24 catch trials (29% of all trials, each condition had 6 catch trials) with

comprehension questions regarding the scripts were included. In each catch trial, a triangle was presented at the center after the ratings for a jitter duration of 0.5–1.5 s followed by a Yes/No comprehension question, and participants were asked to answer the comprehension question by pressing the corresponding button.

Data analyses

Two lesion control participants, who had lesions in the left insula and left temporal cortex respectively, and 3 healthy control participants were excluded from the data analyses because their accuracies for either the performer judgments or the comprehension questions were below 2 standard deviation from the mean.

Analyses of performances of the performer judgments and the comprehension questions

To assess the participants' abilities to perform the experimental tasks, we calculated the response rates as the percentage of responded trials for the performer judgments and the comprehension questions, respectively. We tested the differences in accuracies of the 2 questions between the groups using one-way analysis of variance (ANOVA).

Bayesian hierarchical logistic models

To assess the extent to which communicative functions could be predicted by the speaker's will and the addressee's will, we

fitted Bayesian hierarchical logistic models for "*Promise* vs. *Reply-1*" and "*Request* vs. *Reply-2*" respectively using *Stan* (Carpenter et al. 2017) in R. To exclude trials with scripts that were apparently not comprehended by the participants, the model-fitting only used the trials with correct performer judgments, leaving 91% of the data. The communicative function was included as the response variable, the ratings of the speaker's will and of the addressee's will were included as the predictors, and the age of the participants was included as a covariate to regress out the variance of the age, as shown in Eq. (4).

$$logit(communicative\ function) = b_{i1} \cdot speakers\ will + b_{i2} \cdot addressees\ will$$
$$+ b_3 \cdot age + b_{i0} + e_i \qquad (4)$$

In each hierarchical logistic model fitted with logit function, the slopes of the speaker's will rating and the addressee's will rating and the intercept were estimated at the group-level and the participant-level, respectively. The group-level analysis independently estimated the parameters for each group and tested the effect estimates of the ratings within each of the 3 independent groups. The participant-level analysis independently estimated the parameters for each participant and tested the difference in the estimates between the groups. Each group-level parameter had a normal prior distribution, which had a mean with a prior of *Normal(0,100)* and a standard deviation with a prior of *Cauchy(0,5)*. Each of the participant-level parameters also had a normal prior distribution, which had a mean equaling to the mean of the corresponding group-level distribution and a standard deviation with a prior of *Cauchy(0,5)*. These parameters were shown in Eq. (4), for the ith participant, with the slopes of the 2 ratings, b_{i1} and b_{i2}, and the intercept, b_{i0}. The model also included b_3 as the slope of the participants' age and e_i as the ith participant's residual. Each of these parameters had a normal prior distribution, which had a mean with a prior of *Normal(0,100)* and a standard deviation with a prior of *Cauchy(0,5)*. The model-fitting method was the same as the analysis of the ratings in the fMRI study. All posterior estimates reported have $\hat{R}$ lower than 1.01.

Furthermore, we conducted Frequentist *t*-tests and Bayesian *t*-tests to compare the participant-level posterior estimates of the ratings between the groups. *T*-statistics, Cohen's *d*-values, *P*-values, and Bayes factors in supporting H$_1$ against H$_0$, BF$_{10}$, are reported in Results. To test the linear trend of the participant-level estimates across groups, we fitted linear regression models that included these estimates as response variables and the group as the predictor, with the premotor lesion patients coded as 1, lesion controls coded as 2, and healthy controls coded as 3. The slopes for the groups, *b*, the corresponding *t*-statistics, *P*-values, and the Bayes factors BF$_{10}$ against the intercept-only models are reported in *Results*.

Results
Study 1: fMRI study
Behavioral results

For the results of the pilot evaluation, Bayesian logistic mixed models showed higher ratings of addressee's will, cost–benefit, and pleasure for *Promise* than for *Reply-1*, and higher ratings of speaker's will, cost–benefit, and pleasure for *Request* than for *Reply-2* (Supplemental Fig. S2a and Table S2). The EFA revealed 3 accounting factors: the speaker's attitudes, covering speaker's will, cost–benefit, and pleasure; the addressee's attitudes, covering addressee's will, cost–benefit, and pleasure; and contextual information, covering relative power, social distance, and mitigation (Supplemental Fig. S2b). The feature of the performer's capability had loadings lower than 0.3 on any of the 3 accounting factors and hence was not considered as explainable by either factor. Please see Supplemental Information for the statistics of these results.

The same pattern of rating results as the pilot evaluation were obtained from the post-scanning ratings. Bayesian logistic mixed models were applied on the post-scanning ratings to estimate model coefficients of the features in predicting the pair-wise communicative functions, "*Promise* vs. *Reply-1*" and "*Request* vs. *Reply-2*", respectively (Supplemental Fig. 1b and Table S2). Results showed that, for "*Promise* vs. *Reply-1*", the ratings of addressee's will, cost–benefit, and pleasure were higher for *Promise* than for *Reply-1* while the ratings of speaker's cost–benefit and social distance were lower for *Promise* than for *Reply-1*; for "*Request* vs. *Reply-2*", the ratings of speaker's will, cost–benefit, and pleasure and relative power were higher for *Request* than for *Reply-2* while the ratings of addressee's will, cost–benefit, and pleasure and mitigation were lower for *Request* than for *Reply-2*. A further CFA on the post-scanning ratings was conducted to confirm the appropriateness of the 3-factor model obtained by the above EFA and to show a good fit of the 3-factor model (Fig. 1c; CFI = 0.92, TLI = 0.88, RMSEA = 0.11).

Multivariate pattern classification results of fMRI data

ROI-based MVPCs were conducted to test if the different communicative functions induced distinct activity patterns. As shown in Figure 2b, for "*Promise* vs. *Reply-1*", classification accuracies were above chance level in all ROIs (all *P*-values < 0.0005, permutation-based significance testing with Bonferroni corrections for multiple comparisons, Table 2). For "*Request* vs. *Reply-2*", accuracies were also above chance level in all ROIs (all *P*-values < 0.0005). For "*Promise* vs. *Request*," accuracies were above chance level in all ROIs (all *P*-values < 0.0005) except LSTG. For "*Reply-1* vs. *Reply-2*", the accuracy was above chance only in MPMC (*P*-value < 0.0005).

To examine whether the premotor cortex represented more information on communicative functions than the perisylvian regions, we conducted combinatorial MVPCs (Clithero et al. 2009; Carter et al. 2012). This was implemented by quantifying the extent to which an added ROI improved the classification accuracy of an initial ROI. At the first step, using one of the perisylvian ROIs as the initial ROI and either LPMC or MPMC as the added ROI, we showed that the accuracies in classifying "*Promise* vs. *Reply-1*" (Fig. 2c left panel and Table 2) were significantly improved by adding LPMC, or by adding MPMC. The accuracies in classifying "*Request* vs. *Reply-2*" (Fig. 2c right panel and Table 2) were also significantly improved by adding LPMC or MPMC.

At the second step, we compared the improvements in classification contributed by the premotor cortex with the improvements contributed by the perisylvian regions. For "*Promise* vs. *Reply-1*" (Fig. 2c left panel and Table 2), the results showed that the improvement contributed by LPMC for either of the perisylvian ROIs (except LMTG) was larger than the improvement contributed by either of the perisylvian ROIs for LPMC (left BA44: 18% vs. 8%; left BA45: 21% vs. 5%; LSTG: 13% vs. 4%, all *P*-values < 0.0005); the improvement contributed by MPMC for either of the perisylvian ROIs was larger than the improvement contributed by either of the perisylvian ROIs for MPMC (left BA44: 22% vs. 5%; left BA45: 26% vs. 4%; LMTG: 10% vs. 5%; LSTG: 17% vs. 1%, all *P*-values < 0.0005).

For "*Request* vs. *Reply-2*" (Fig. 2c right panel and Table 2), the same pattern of results was observed on the improvements contributed by LPMC for all the perisylvian ROIs (left BA44: 17% vs.

Table 2. MVPC results of fMRI data.

ROI-based MVPCs

ROI (n voxels)	Index	Pair-wise classification			
		Promise vs. Reply-1	Request vs. Reply-2	Promise vs. Request	Reply-1 vs. Reply-2
LPMC (5507)	Accuracy (%)	60	67	55	50
	P	<0.0005	<0.0005	<0.0005	0.534
MPMC (5227)	Accuracy (%)	64	67	58	58
	P	<0.0005	<0.0005	<0.0005	<0.0005
Left BA44 (1443)	Accuracy (%)	56	58	55	51
	P	<0.0005	<0.0005	<0.0005	0.128
Left BA45 (979)	Accuracy (%)	53	58	58	49
	P	<0.0005	<0.0005	<0.0005	0.827
LMTG (1760)	Accuracy (%)	61	60	55	51
	P	<0.0005	<0.0005	<0.0005	0.078
LSTG (1147)	Accuracy (%)	56	57	51	51
	P	<0.0005	<0.0005	0.018	0.028

Combinatorial MVPCs of Δaccuracy (initial ROI, added ROI)

Pair-wise classification	Premotor ROI	Perisylvian ROI	Δaccuracy (perisylvian ROI, premotor ROI)		Δaccuracy (premotor ROI, perisylvian ROI)		Difference between Δaccuracies	
			Δaccuracy (%)	P	Δaccuracy (%)	P	Δaccuracy (%)	P
Promise vs. Reply-1	LPMC	Left BA44	18	<0.0005	**8**	<0.0005	10	<0.0005
		Left BA45	21	<0.0005	**5**	<0.0005	16	<0.0005
		LMTG	4	0.0015	**5**	<0.0005	−1	0.5
		LSTG	13	<0.0005	4	0.0045	9	<0.0005
	MPMC	Left BA44	22	<0.0005	**5**	<0.0005	17	<0.0005
		Left BA45	26	<0.0005	**4**	0.001	22	<0.0005
		LMTG	10	<0.0005	**5**	<0.0005	5	<0.0005
		LSTG	17	<0.0005	1	0.1565	16	<0.0005
Request vs. Reply-2	LPMC	Left BA44	17	<0.0005	4	0.002	12	<0.0005
		Left BA45	15	<0.0005	3	0.0115	12	<0.0005
		LMTG	13	<0.0005	3	0.0055	10	<0.0005
		LSTG	16	<0.0005	2	0.0725	14	<0.0005
	MPMC	Left BA44	17	<0.0005	**5**	<0.0005	12	<0.0005
		Left BA45	15	<0.0005	**4**	0.0015	11	<0.0005
		LMTG	14	<0.0005	**5**	<0.0005	9	<0.0005
		LSTG	16	<0.0005	3	0.01	13	<0.0005

Texts in bold indicate statistical significance for the permutation-based significance testing with Bonferroni correction. For ROI-based MVPCs, accuracies were tested with Bonferroni corrected significance threshold of $P < 0.002$. For combinatorial MVPCs, statistical significances for the permutation tests at the first step and the second step were determined by Bonferroni corrected thresholds of $P < 0.0016$ and $P < 0.003$, respectively. LPMC, lateral premotor cortex; MPMC, medial premotor cortex; Left BA44, Broca's area (BA44); Left BA45, Broca's area (BA45); LMTG, Left middle temporal gyrus; LSTG, Left superior temporal gyrus.

4%; left BA45: 15% vs. 3%; LMTG: 13% vs. 3%; LSTG: 16% vs. 2%, all *P*-values < 0.0005); and on the improvements contributed by the MPMC (left BA44: 17% vs. 5%; left BA45: 15% vs. 4%; LMTG: 14% vs. 5%; LSTG: 16% vs. 3%, all *P*-values < 0.0005).

In addition, as the medial prefrontal cortex (MPFC) and temporo-parietal junction (TPJ) were shown to activate in processing linguistic communications in previous studies (e.g. indirect reply) (Shibata et al. 2011; Feng et al. 2017, 2021), we compared the amount of information on communicative functions represented in the premotor cortex with the amount of information represented in the MPFC and TPJ, using the same methods illustrated above (Supplemental Information). The results suggested that, although the MPFC and TPJ represented information on communicative functions to a certain extent, the premotor cortex represented more (Supplemental Fig. S5 and Table S4).

Taken together, the MVPC results suggested that while both the premotor cortex and the perisylvian regions contain information on communicative functions, the premotor cortex represented more information relative to the perisylvian regions and other brain areas previously shown to be related to linguistic communications.

Representational similarity analysis results of fMRI data

As shown by the rating results, communicative functions were related to the interlocutor-related features. We thus conducted RSA (Kriegeskorte et al. 2008) to examine the extent to which the activation pattern in the premotor cortex and in the perisylvian regions could be predicted by the 3 behavioral accounting factors (speaker's attitudes, addressee's attitudes, and contextual information), and vice versa.

First, the results of the RS encoding models showed that, for "*Promise* vs. *Reply-1*" (Fig. 3c upper panel and Table 3), each brain RDM was significantly predicted by Addressee RDM, but not by Speaker RDM or Context RDM. For "*Request* vs. *Reply-2*" (Fig. 3c lower panel and Table 3), brain RDMs of LPMC, MPMC, left BA44, LMTG, and LSTG were significantly predicted by Speaker RDM, but not by Addressee RDM or Context RDM. However, no significant effect was observed for left BA45 RDM.

Second, the results of the RS decoding models showed that, for "*Promise* vs. *Reply-1*" (Fig. 3e upper panel and Table 3), Addressee RDM was predicted by LPMC RDM or MPMC RDM. In the MPMC model, Addressee RDM was also predicted by LMTG RDM, while the mean estimate of the model coefficient of MPMC RDM was numerically higher than that of LMTG RDM (0.3 vs. 0.11). In contrast, neither Speaker RDM nor Context RDM was predicted by any of the brain RDMs (Supplemental Fig. S7 and Table S6). For "*Request* vs. *Reply-2*" (Fig. 3e lower panel and Table 3), Speaker RDM was predicted by LPMC RDM. In contrast, neither Addressee RDM nor Context RDM were predicted by any of the brain RDMs (Supplemental Fig. S7 and Table S6).

Thus, in an extension of the MVPC results, the RSA results suggested that, relative to the perisylvian regions, the premotor cortex more robustly represents *Promise*-related information that is predicted by the addressee's attitudes, and *Request*-related information that is predicted by the speaker's attitudes.

Study 2: lesion study
Performance on the performer judgments and the comprehension questions

For the comprehension questions, 2 premotor lesion patients had response rates of 96% and 98% respectively, one lesion control patient had a response rate of 99%, and 3 healthy participants had

response rates of 99%, 99%, and 95% respectively. Apart from that, all participants showed a response rate of 100% for the performer judgments. All participants had response rate of 100% for the comprehension questions. These response rates indicated that all participants were capable of manually performing the tasks.

As shown in Supplemental Table S7, average accuracies of the performer judgments were 89%, 94%, and 90% and that of the comprehension questions were 76%, 79%, and 84% for premotor lesion patients, lesion controls, and healthy controls respectively. Results of one-way ANOVA comparing the accuracies between the groups showed no significant effect (all *P*-values > 0.1). These results indicated that the participants' engagement in reading the scripts and that the 3 groups had comparable performances for the 2 questions.

Results of Bayesian hierarchical logistic models

Bayesian hierarchical logistic models were fitted to estimate parameters at both the group-level and the participant-level. For "*Promise* vs. *Reply-1*" model (Fig. 4c upper panel and Supplemental Table S5), the group-level results showed that communicative functions were significantly predicted by the addressee's will rating for both lesion controls and healthy controls ($b = 1.19$, 95% CrI: [0.43, 1.99]; $b = 1.89$, 95% CrI: [1.33, 2.5], respectively), but not for the premotor lesion patients ($b = 0.68$, 95% CrI: [−0.05, 1.43]). For all groups, no significant predictability of the speaker's will rating was observed. For the differences between the groups in the predictability of the addressee's will rating, pair-wise comparisons on the participant-level estimates were performed. Each comparison of the participant-level posterior estimates between 2 groups tested the null hypothesis (H_0), "there was no difference in the estimates between the groups," against the alternative hypothesis (H_1), "there was a difference in the estimates between the groups". The results showed that the predictability of the addressee's will rating for the premotor lesion patients was significantly lower than that for healthy controls (0.69 vs. 1.89, $t_{(38.62)} = −3.76$, Cohen's $d = 1.13$, $P < 0.001$), with Bayes factor $BF_{10} = 13$, suggesting strong evidence for this difference (according to Andraszewicz et al.' (2015) suggestion, a BF_{10} between 10 and 30 indicates strong evidence for H_1, and a BF_{10} between 0.33 and 1 indicates anecdotal evidence for H_0). In contrast, there were no reliable difference between the predictability of the addressee's will ratings for lesion controls and for healthy controls (1.19 vs. 1.89, $t_{(24.38)} = −1.61$, Cohen's $d = 0.54$, $P = 0.12$), with Bayes factor $BF_{10} = 0.86$. As the pattern of the participant-level estimates of the predictability of the addressee's will ratings showed the lowest mean value for the premotor lesion patients and the highest mean value for healthy controls, further linear regression modeling was performed to test the linear trend of these estimates across the groups, with the premotor lesion patients, lesion controls, and healthy controls coded as 1, 2, and 3, respectively. The result showed a significant positive slope for the groups ($\beta = 0.61$, $t = 3.21$, $P = 0.002$, $BF_{10} = 15.63$), suggesting that the comprehensibility of communication functions for *Promise* (vs. *Reply-1*) can be increasingly predicted by the addressee's will rating over the 3 groups.

For "*Request* vs. *Reply-2*" (Fig. 4c lower panel and Table S5), the results of the group-level estimates showed that communicative functions were significantly predicted by the speaker's will rating for both lesion controls and healthy controls ($b = 0.85$, 95% CrI: [0.17, 1.59]; $b = 1.38$, 95% CrI: [0.89, 1.92], respectively), but not for the premotor lesion patients ($b = 0.44$, 95% CrI: [−0.21, 1.09]). For all groups, "*Request* vs. *Reply-2*" were predicted by the addressee's

Table 3. RSA results of fMRI data.

Representational similarity encoding model

| | | Behavioral RDM | | | | | |
| | | Speaker | | Addressee | | Context | |
ROI	Prediction	b	99.86% CrI	b	99.86% CrI	b	99.86% CrI
LPMC	Promise vs. Reply-1	−0.001	[−0.003, 0.001]	**0.007**	**[0.004, 0.01]**	0.0003	[−0.002, 0.003]
	Request vs. Reply-2	**0.004**	**[0.002, 0.007]**	0.001	[−0.001, 0.004]	0.001	[−0.002, 0.003]
MPMC	Promise vs. Reply-1	−0.001	[−0.003, 0.002]	**0.007**	**[0.004, 0.01]**	−0.0003	[−0.003, 0.003]
	Request vs. Reply-2	**0.004**	**[0.002, 0.006]**	0.001	[−0.002, 0.004]	0.001	[−0.002, 0.003]
Left BA44	Promise vs. Reply-1	0.0001	[−0.003, 0.003]	**0.005**	**[0.002, 0.008]**	−0.0001	[−0.004, 0.004]
	Request vs. Reply-2	**0.005**	**[0.002, 0.009]**	0.001	[−0.003, 0.004]	−0.001	[−0.004, 0.002]
Left BA45	Promise vs. Reply-1	0.001	[−0.002, 0.005]	**0.005**	**[0.002, 0.008]**	−0.002	[−0.006, 0.003]
	Request vs. Reply-2	0.003	[−0.004, 0.007]	0.0003	[−0.004, 0.004]	0.001	[−0.003, 0.005]
LMTG	Promise vs. Reply-1	−0.001	[−0.004, 0.002]	**0.006**	**[0.003, 0.009]**	0.00002	[−0.003, 0.003]
	Request vs. Reply-2	**0.004**	**[0.001, 0.007]**	−0.0001	[−0.003, 0.003]	0.001	[−0.002, 0.005]
LSTG	Promise vs. Reply-1	−0.0005	[−0.004, 0.002]	**0.005**	**[0.002, 0.008]**	−0.001	[−0.004, 0.003]
	Request vs. Reply-2	**0.005**	**[0.001, 0.01]**	−0.001	[−0.004, 0.003]	0.0003	[−0.003, 0.004]

Representational similarity decoding model

| | | | ROI | | | | | | | | | |
| | | | LPMC/MPMC | | Left BA44 | | Left BA45 | | LMTG | | LSTG | |
Prediction	Model	Behavioral RDM	b	99.92% CrI	b	99.92% CrI	b	99.92% CrI	b	99.92% CrI	b	99.92% CrI
Promise vs. Reply-1	LPMC model	Addressee	**0.34**	**[0.12, 0.55]**	0.002	[−0.1, 0.11]	0.02	[−0.08, 0.13]	0.11	[−0.0001, 0.11]	0.02	[−0.12, 0.15]
	MPMC model		**0.3**	**[0.08, 0.53]**	0.008	[−0.1, 0.12]	0.03	[−0.08, 0.14]	**0.11**	**[0.002, 0.23]**	0.02	[−0.11, 0.15]
Request vs. Reply-2	LPMC model	Speaker	**0.29**	**[0.01, 0.38]**	0.08	[−0.06, 0.22]	−0.03	[−0.01, 0.05]	0.05	[−0.06, 0.16]	0.04	[−0.1, 0.16]
	MPMC model		0.12	[−0.03, 0.27]	0.09	[−0.05, 0.22]	−0.03	[−0.11, 0.06]	0.05	[−0.06, 0.16]	0.04	[−0.08, 0.16]

Texts in bold indicate statistical significance with Bonferroni corrected CrI (99.86% CrI for the encoding models; 99.92% CrI for the decoding models). LPMC, lateral premotor cortex; MPMC, medial premotor cortex; Left BA44, Broca's area (BA44); Left BA45, Broca's area (BA45); LMTG, Left middle temporal gyrus; LSTG, Left superior temporal gyrus

will ratings. For the differences between the groups in the predictability of the speaker's will rating, further comparisons on the participant-level estimates were performed. The results showed that the predictability of the speaker's will rating for the premotor lesion patients was significantly lower than that for healthy controls (0.44 vs. 1.38, $t_{(38.4)} = -3.64$, Cohen's $d = 1.1$, $P < 0.001$), with Bayes factor $BF_{10} = 10.92$, suggesting strong evidence for this difference. In contrast, there was no reliable difference between the predictability of the speaker's will rating for lesion controls and that for healthy controls (0.85 vs. 1.38, $t_{(22.26)} = -1.41$, Cohen's $d = 0.48$, $P = 0.17$), with Bayes factor $BF_{10} = 0.73$. As the pattern of the participant-level estimates of the predictability of the speaker's will ratings showed the lowest mean value for the premotor lesion patients and the highest mean value for healthy controls, further linear regression modeling was performed to test the linear trend of these estimates across the groups. The result showed a significant positive slope for the groups ($\beta = 0.48$, $t = 3.03$, $P = 0.004$, $BF_{10} = 10.29$), suggesting that the comprehensibility of the communication functions for *Request* (vs. *Reply-2*) can be increasingly predicted by the speaker's will rating over the 3 groups.

Taken together, these results suggested that patients with lesions in the premotor cortex were impaired in comprehending communicative functions as compared with healthy controls. In contrast, there was no reliable difference between patients with lesions in brain regions other than the premotor cortex and healthy controls.

Discussion

Across 2 studies, our results consistently and convergently demonstrated the role of the premotor cortex in representing linguistic communicative functions. The MVPC results showed that both the premotor cortex and the perisylvian regions contain information on communicative functions, and the results of the RS encoding models showed that the function-related activity in these areas could be predicted by the interlocutors' attitudes. These findings suggest that understanding linguistic communicative functions involves both the premotor cortex and the perisylvian regions. Moreover, the results of combinatorial MVPCs showed that the premotor cortex is more sensitive than the perisylvian regions to communicative functions, and the results of the RS decoding model showed that the function-related activity in the premotor cortex is more reliably related to the interlocutors' attitudes than that in the perisylvian regions. These findings suggest that the premotor cortex is more pronounced in representing communicative functions than the perisylvian regions. Furthermore, in the lesion study, the results of both the comparisons of the participant-level estimates between the groups and the linear trend analyses showed that, the predictability of the speaker/addressee's will ratings has the lowest value for patients with premotor lesions, the medium value for lesion controls, and the highest value for healthy controls. These results suggest that the premotor cortex lesions have profoundly impaired the understanding of communicative functions, demonstrating a causal role of the premotor cortex in representing these functions. Although we did not have a perisylvian lesion group to examine the potential causal role of the perisylvian regions, the 2 studies together provide evidence for the profound role of the premotor cortex in comprehending linguistic communications. Collectively, the current work supports the theoretical view (Wittgenstein 1953;

Searle 1969; Austin 1975) that linguistic communications are represented as actions in the brain.

In an extension of previous fMRI studies on linguistic communications (Shibata et al. 2011; van Ackeren et al. 2012; Egorova et al. 2016; Feng et al. 2017, 2021), we used sentences that directly convey communicative functions that are independent of particular actions. Specifically, our results showed that the activation patterns in the premotor cortex could discriminate the communicative functions even though the critical sentences (e.g. "I/You will analyze the survey data this week." in Table 1) described the conduct of the same task (e.g. "analyzing the survey data") across all conditions. Thus, these function-related representations go beyond not only action semantics but also representations of particular actions of conducting the tasks. We suggest that the premotor cortex represents the relation between the interlocutors and the information of the speaker's sentence. This relation can be reflected by the interlocutors' attitudes (e.g. the speaker/addressee's will/cost–benefit/pleasure) toward the information of the sentence (Searle and Vanderveken 1985). Specifically, the premotor cortex represents not simply what action would be conducted (e.g. the data analysis) but more importantly the extent to which the interlocutors would like to have the action accomplished. In agreement with this argument, the results of both the RSA and the lesion study demonstrated that the communicative function-related activity pattern in the premotor cortex was related to the specific interlocutor's attitude that predicted the function. Specifically, the premotor cortex was sensitive to the addressee's attitude when discriminating *Promise* from *Reply-1* while sensitive to the speaker's attitude when discriminating *Request* from *Reply-2*. These interlocutors' attitudes clarified the relations between the interlocutors and their intentions toward the communicative action. To bind each interlocutor with an intention, the comprehender can mentally objectify the intention during the processing of the communicative action (Whorf 1941). In a general sense, the interlocutors and the information of the speaker's sentence can be deemed as the subjects and their objectified intentions respectively. Such a generalization echoes with a recent study showing that the training of motor actions improves the understanding of subject-object relations in sentences (Thibault et al. 2021), demonstrating the general role of the motor system in understanding relations between subjects and objects of actions.

To establish the relations between the interlocutors and the sentential information for linguistic communications, the premotor cortex can function in a way like the understanding of motor actions (Rizzolatti et al. 1996; Rizzolatti and Sinigaglia 2016). It has been suggested that the human premotor cortex contains neurons with "mirror" properties (Rizzolatti et al. 1988; Rizzolatti and Arbib 1998) that enable similar activation patterns for action implementation and action observation (Avenanti et al. 2007; Molenberghs et al. 2012; Oosterhof et al. 2012, 2013; Rizzolatti et al. 2014). Specifically, the premotor activity patterns induced by observing others' actions are similar to those induced by implementing actions (Oosterhof et al. 2012). The premotor cortex has been repeatedly shown to be involved in understanding goal-directed motor actions (e.g. reaching or grasping) (Cattaneo et al. 2010; Gallivan, McLean, Smith, et al. 2011a; Gallivan, McLean, Valyear, et al. 2011b; Gallivan et al. 2013; Michael et al. 2014). During the understanding of an observed goal-directed action, the premotor cortex supports a reactivation of the representation of relevant action program, a process termed as action/mental simulation (Gallese and Goldman 1998; Jeannerod 2001; Jacob and Jeannerod 2005; Zwaan 2016). Similarly, the linguistic

communication is represented as the goal-directed action that serve the communicative function. The speaker aims to achieve the goal of having the particular task accomplished. Moreover, during the processing of linguistic materials, the premotor cortex could represent an integration of the focused information and the context. This has been shown by stronger activity in the premotor cortex for narratives containing sentences with coherent meanings than for sentences with unrelated meanings (Xu et al. 2005), as well as for a counterfactual 2-clause sentence conveying competing meanings with the combination of the 2 clauses than for a factual one without such competition (Urrutia et al. 2012). Along this line, in understanding the communicative function such as the cases in the present study, a mental simulation occurs to the comprehender by which a model is built to integrate the conduction of the task with the interlocutors' attitudes; this simulation thus clarifies the relation between the interlocutors and their objectified intentions (Zwaan 2016).

In processing the speaker's meaning in linguistic communication, the comprehender could, on the one hand, mentally simulate the speaker's communicative action, and/or, on the other hand, infer the speaker's meaning and goal using a "theory of mind" about the speaker's (and possibly addressee's) mental state as suggested by previous studies (van Ackeren et al. 2012; Feng et al. 2021). This use of "theory of mind" is generally supported by the increased activations in the MPFC and TPJ (Schurz et al. 2014). Although the current fMRI experiment did observe that these typical "theory of mind" regions represented communicative functions, the strength of the representations in these regions was weaker than that in the premotor cortex. Our findings thus support the notion that understanding communicative functions is a relatively primitive and spontaneous process of projecting one's own experience on the other's action that requires mental simulation rather than more effortful inference based on a "theory" about the other (Gordon 1992; Gallese and Goldman 1998). In many situations this primitive simulation process is sufficient to support the social functions of language (Gallese 2008), including communicating with others (Garrod and Pickering 2004).

Our suggestion of mental simulation in comprehending linguistic communications is in accordance with linguistic pragmatic accounts. Firstly, the idealized cognitive model suggests that each communicative function has a prototypical model that is characterized by several social features, including interlocutors' attitudes (Lakoff 1987; Pérez 2001). As revealed by Pérez's (2001) analysis of the corpus of linguistic communication scenarios, the prototypical model of *Promise* is characterized by high addressee's will and benefit whereas the prototypical model of *Request* is characterized by high speaker's will and benefit. The present results have shown that the premotor cortex represented these interlocutor-related social features during the understanding of the communicative functions. Consistently, previous fMRI studies on communications showed that the premotor cortex represented social information, such as the communicator's intention (Ciaramidaro et al. 2013) and emotion (Warren et al. 2006). We thus suggest that, to identify the function of the linguistic communication, the comprehender builds a model of the communication by mental simulation, then matches the built model with the internal prototypical model. Secondly, the connection between linguistic communication and motor action is also proposed by the action prediction theory of communicative function (Boux et al. 2021; Tomasello et al. 2022). This account considers linguistic communication as an action sequence consisting of the action contained in the speaker's sentence, and the preceding and following actions. During the understanding

of the communicative function, the comprehender predicts the particular following action that would eventually achieve the speaker's goal. Such action prediction is revealed by stronger activities in the motor system for the communicative functions that require the addressee's active responses (e.g. requesting an object and asking a question) than for the functions without this requirement (e.g. naming an object and stating a situation) (Egorova et al. 2016; Tomasello et al. 2019; Boux et al. 2021; Tomasello et al. 2022). These observations fit with our findings concerning the premotor cortex. We further showed that the activity patterns in the premotor cortex could discriminate between different communicative functions, even the same actions were expected to follow the communications. We thus suggest that the action sequence of the communication is built by the mental simulation. In this sense, the prediction of a particular following action is a part of the simulation that involves the motor system. Moreover, the mental simulation of the particular action can also involve the premotor cortex in processing action semantics without explicit communicative functions, such as action verbs (Hauk et al. 2004; Tremblay et al. 2012), suggesting a more general role of the premotor cortex in understanding linguistic communications, rather than in representing the specific action.

The shared mechanisms of mental simulation for language comprehension and motor action understanding is likely to be the evolutionary consequence of communicating with each other in a symbolic or language-like manner. While both symbolic communicative actions and tool-using (Gallivan et al. 2013) are intellectual behaviors shared by humans and nonhuman primates (Seyfarth et al. 1980; Arnold and Zuberbühler 2006; Seed and Byrne 2010; Watson Stuart et al. 2015), the connectivity between the left posterior temporal cortex and the left inferior frontal cortex in the perisylvian area is weaker in nonhuman primates' brain than in the human brain (Friederici 2009; Balezeau et al. 2020). Taken together, the premotor region might serve more as a footstone of the co-evolution of humans' linguistic ability and tool-using/making skills than the perisylvian regions (Arbib 2011; Stout and Chaminade 2012). As the current study was based only on human subjects, it is thus for future studies to investigate this issue.

To conclude, while both the premotor cortex and the perisylvian language regions represent the information on communicative functions and the interlocutors' attitudes, the premotor cortex represents more information than the perisylvian regions. Moreover, lesions in the premotor cortex result in impaired processing of linguistic communications. These findings demonstrated that the premotor cortex is necessary for comprehending communicative functions in language processing, supporting the theoretical view that linguistic communications are represented as actions in the brain.

Authors' contributions

WC and XZ designed the experiments. WC, RY, XW, and ZG conducted the experiments. WC and LW analyzed the data. WC, LW, and XZ wrote the paper. WC, LW, RY, XW, ZG, and XZ revised the paper.

Acknowledgements

Supplementary material

Supplementary material is available at *Cerebral Cortex* online.

Funding

Conflict of interest statement: The authors declare no conflict of interest.

References

Amunts K, Schleicher A, Bürgel U, Mohlberg H, Uylings HBM, Zilles K. Broca's region revisited: cytoarchitecture and intersubject variability. *J Comp Neurol*. 1999:412:319–341.

Andraszewicz S, Scheibehenne B, Rieskamp J, Grasman R, Verhagen J, Wagenmakers E-J. An introduction to Bayesian hypothesis testing for management research. *J Manag*. 2015:41:521–543.

Arbib MA. From mirror neurons to complex imitation in the evolution of language and tool use. *Annu Rev Anthropol*. 2011:40:257–273.

Arbib MA. Towards a computational comparative neuroprimatology: framing the language-ready brain. *Phys Life Rev*. 2016:16:1–54.

Arnold K, Zuberbühler K. Semantic combinations in primate calls. *Nature*. 2006:441:303–303.

Austin JL. *How to do things with words*. Cambridge, MA: Harvard University Press; 1975.

Avenanti A, Bolognini N, Maravita A, Aglioti SM. Somatic and motor components of action simulation. *Curr Biol*. 2007:17:2129–2135.

Aziz-Zadeh L, Koski L, Zaidel E, Mazziotta J, Iacoboni M. Lateralization of the human mirror neuron system. *J Neurosci*. 2006:26:2964–2970.

Balezeau F, Wilson B, Gallardo G, Dick F, Hopkins W, Anwander A, Friederici AD, Griffiths TD, Petkov CI. Primate auditory prototype in the evolution of the arcuate fasciculus. *Nat Neurosci*. 2020:23:611–614.

Barr DJ, Levy R, Scheepers C, Tily HJ. Random effects structure for confirmatory hypothesis testing: keep it maximal. *J Mem Lang*. 2013:68:255–278.

Battaglini M, Jenkinson M, De Stefano N. Evaluating and reducing the impact of white matter lesions on brain volume measurements. *Hum Brain Mapp*. 2012:33:2062–2071.

Bianchi S, Reyes LD, Hopkins WD, Taglialatela JP, Sherwood CC. Neocortical grey matter distribution underlying voluntary, flexible vocalizations in chimpanzees. *Sci Rep*. 2016:6:34733.

Boux I, Tomasello R, Grisoni L, Pulvermüller F. Brain signatures predict communicative function of speech production in interaction. *Cortex*. 2021:135:127–145.

Brainard DH. The psychophysics toolbox. *Spat Vis*. 1997:10:433–436.

Brennan SE, Galati A, Kuhlen AK. Chapter 8—two minds, one dialog: coordinating speaking and understanding. In: Ross BH, editors. *Psychology of learning and motivation*. San Diego, CA: Academic Press; 2010. pp. 301–344

Bürkner P-C. brms: an R package for bayesian multilevel models using stan. *J Stat Softw*. 2017:80:1–28.

Carpenter B, Gelman A, Hoffman MD, Lee D, Goodrich B, Betancourt M, Brubaker M, Guo J, Li P, Riddell A. Stan: a probabilistic programming language. *J Stat Softw*. 2017:76:1–32.

Carter RM, Bowling DL, Reeck C, Huettel SA. A distinct role of the temporal-parietal junction in predicting socially guided decisions. *Science*. 2012:337:109–111.

Cattaneo L, Barchiesi G, Tabarelli D, Arfeller C, Sato M, Glenberg AM. One's motor performance predictably modulates the understanding of others' actions through adaptation of premotor visuo-motor neurons. *Soc Cogn Affect Neurosci*. 2010:6:301–310.

Ciaramidaro A, Becchio C, Colle L, Bara BG, Walter H. Do you mean me? Communicative intentions recruit the mirror and the mentalizing system. *Soc Cogn Affect Neurosci*. 2013:9:909–916.

Clithero JA, Carter RM, Huettel SA. Local pattern classification differentiates processes of economic valuation. *NeuroImage*. 2009:45:1329–1338.

Courson M, Macoir J, Tremblay P. Role of medial premotor areas in action language processing in relation to motor skills. *Cortex*. 2017:95:77–91.

Desikan RS, Ségonne F, Fischl B, Quinn BT, Dickerson BC, Blacker D, Buckner RL, Dale AM, Maguire RP, Hyman BT et al. An automated labeling system for subdividing the human cerebral cortex on MRI scans into gyral based regions of interest. *NeuroImage*. 2006:31:968–980.

Dreyer FR, Pulvermüller F. Abstract semantics in the motor system? An event-related fMRI study on passive reading of semantic word categories carrying abstract emotional and mental meaning. *Cortex*. 2018:100:52–70.

Egorova N, Shtyrov Y, Pulvermüller F. Brain basis of communicative actions in language. *NeuroImage*. 2016:125:857–867.

Feng W, Wu Y, Jan C, Yu H, Jiang X, Zhou X. Effects of contextual relevance on pragmatic inference during conversation: an fMRI study. *Brain Lang*. 2017:171:52–61.

Feng W, Yu H, Zhou X. Understanding particularized and generalized conversational implicatures: is theory-of-mind necessary? *Brain Lang*. 2021:212:104878.

Friederici AD. Pathways to language: fiber tracts in the human brain. *Trends Cogn Sci*. 2009:13:175–181.

Friederici AD. The brain basis of language processing: from structure to function. *Physiol Rev*. 2011:91:1357–1392.

Friederici AD, Chomsky N, Berwick RC, Moro A, Bolhuis JJ. Language, mind and brain. *Nat Hum Behav*. 2017:1:713–722.

Gallese V. Mirror neurons and the social nature of language: the neural exploitation hypothesis. *Soc Neurosci*. 2008:3:317–333.

Gallese V, Goldman A. Mirror neurons and the simulation theory of mind-reading. *Trends Cogn Sci*. 1998:2:493–501.

Gallese V, Lakoff G. The brain's concepts: the role of the sensory-motor system in conceptual knowledge. *Cogn Neuropsychol*. 2005:22:455–479.

Gallivan JP, McLean DA, Smith FW, Culham JC. Decoding effector-dependent and effector-independent movement intentions from human parieto-frontal brain activity. *J Neurosci*. 2011a:31:17149–17168.

Gallivan JP, McLean DA, Valyear KF, Pettypiece CE, Culham JC. Decoding action intentions from preparatory brain activity in human parieto-frontal networks. *J Neurosci*. 2011b:31:9599–9610.

Gallivan JP, McLean DA, Valyear KF, Culham JC. Decoding the neural mechanisms of human tool use. *elife*. 2013:2:e00425.

Garrod S, Pickering MJ. Why is conversation so easy? *Trends Cogn Sci*. 2004:8:8–11.

Gelman A, Rubin DB. Inference from iterative simulation using multiple sequences. *Stat Sci*. 1992:7:457–472.

Geyer S. *The microstructural border between the motor and the cognitive domain in the human cerebral cortex*. Berlin, Heidelberg: Springer; 2004

Gil-da-Costa R, Martin A, Lopes MA, Muñoz M, Fritz JB, Braun AR. Species-specific calls activate homologs of Broca's and Wernicke's areas in the macaque. *Nat Neurosci*. 2006:9:1064–1070.

Gordon RM. The simulation theory: objections and misconceptions. *Mind Lang*. 1992:7:11–34.

Hagoort P. The core and beyond in the language-ready brain. *Neurosci Biobehav Rev*. 2017:81:194–204.

Hamilton MC, Schutte NS, M MJ. Hamilton anxiety scale (HAMA). In: *Sourcebook of adult assessment: applied clinical psychology*. New York, NY: Springer; 1976. pp. 154–157

Hanke M, Halchenko YO, Sederberg PB, Hanson SJ, Haxby JV, Pollmann S. PyMVPA: a Python toolbox for multivariate pattern analysis of fMRI data. *Neuroinformatics*. 2009:7:37–53.

Hauk O, Johnsrude I, Pulvermüller F. Somatotopic representation of action words in human motor and premotor cortex. *Neuron*. 2004:41:301–307.

Hellbernd N, Sammler D. Neural bases of social communicative intentions in speech. *Soc Cogn Affect Neurosci*. 2018:13:604–615.

Hertrich I, Dietrich S, Ackermann H. The role of the supplementary motor area for speech and language processing. *Neurosci Biobehav Rev*. 2016:68:602–610.

Jacob P, Jeannerod M. The motor theory of social cognition: a critique. *Trends Cogn Sci*. 2005:9:21–25.

Jeannerod M. Neural simulation of action: a unifying mechanism for motor cognition. *NeuroImage*. 2001:14:103–109.

Jenkinson M, Smith S. A global optimisation method for robust affine registration of brain images. *Med Image Anal*. 2001:5:143–156.

Jenkinson M, Bannister P, Brady M, Smith S. Improved optimization for the robust and accurate linear registration and motion correction of brain images. *NeuroImage*. 2002:17:825–841.

Jenkinson M, Beckmann CF, Behrens TEJ, Woolrich MW, Smith SM. FSL. *NeuroImage*. 2012:62:782–790.

Knight RG. Some general population norms for the short form Beck Depression Inventory. *J Clin Psychol*. 1984:40:751–753.

Kriegeskorte N, Mur M, Bandettini P. Representational similarity analysis—connecting the branches of systems neuroscience. *Front Syst Neurosci*. 2008:2:4.

Lakoff G. *Women, fire, and dangerous things: what categories reveal about the mind*. Chicago, IL: University of Chicago Press; 1987

Levinson SC. Turn-taking in human communication—origins and implications for language processing. *Trends Cogn Sci*. 2016:20:6–14.

Lewandowski D, Kurowicka D, Joe H. Generating random correlation matrices based on vines and extended onion method. *J Multivar Anal*. 2009:100:1989–2001.

Li X. The distribution of left and right handedness in Chinese people (中国人的左右利手分布). *Acta Psychol Sin* (心理学报). 1983:3:268–276.

Mayka MA, Corcos DM, Leurgans SE, Vaillancourt DE. Three-dimensional locations and boundaries of motor and premotor cortices as defined by functional brain imaging: a meta-analysis. *NeuroImage*. 2006:31:1453–1474.

Michael J, Sandberg K, Skewes J, Wolf T, Blicher J, Overgaard M, Frith CD. Continuous theta-burst stimulation demonstrates a causal role of premotor homunculus in action understanding. *Psychol Sci*. 2014:25:963–972.

Molenberghs P, Cunnington R, Mattingley JB. Brain regions with mirror properties: a meta-analysis of 125 human fMRI studies. *Neurosci Biobehav Rev*. 2012:36:341–349.

Morgan TJH, Uomini NT, Rendell LE, Chouinard-Thuly L, Street SE, Lewis HM, Cross CP, Evans C, Kearney R, de la Torre I et al. Experimental evidence for the co-evolution of hominin tool-making teaching and language. *Nat Commun*. 2015:6:6029.

Oberski D. lavaan.survey: an R package for complex survey analysis of structural equation models. *J Stat Softw*. 2014:57:1–27.

Oosterhof NN, Tipper SP, Downing PE. Viewpoint (in)dependence of action representations: an MVPA study. *J Cogn Neurosci*. 2012:24:975–989.

Oosterhof NN, Tipper SP, Downing PE. Crossmodal and action-specific: neuroimaging the human mirror neuron system. *Trends Cogn Sci*. 2013:17:311–318.

Pelli DG. The VideoToolbox software for visual psychophysics: transforming numbers into movies. *Spat Vis*. 1997:10:437–442.

Pérez HL. *Illocution and cognition: a constructional approach*. La Rioja. España: Servicio de Publicaciones Universidad de La Rioja; 2001

Pilgramm S, de Haas B, Helm F, Zentgraf K, Stark R, Munzert J, Krüger B. Motor imagery of hand actions: decoding the content of motor imagery from brain activity in frontal and parietal motor areas. *Hum Brain Mapp*. 2016:37:81–93.

Postle N, McMahon KL, Ashton R, Meredith M, de Zubicaray GI. Action word meaning representations in cytoarchitectonically defined primary and premotor cortices. *NeuroImage*. 2008:43:634–644.

Pulvermüller F. Brain mechanisms linking language and action. *Nat Rev Neurosci*. 2005:6:576–582.

Pulvermüller F. Neural reuse of action perception circuits for language, concepts and communication. *Prog Neurobiol*. 2018:160:1–44.

Pulvermüller F, Fadiga L. Active perception: sensorimotor circuits as a cortical basis for language. *Nat Rev Neurosci*. 2010:11:351–360.

Rizzolatti G, Arbib MA. Language within our grasp. *Trends Neurosci*. 1998:21:188–194.

Rizzolatti G, Sinigaglia C. The mirror mechanism: a basic principle of brain function. *Nat Rev Neurosci*. 2016:17:757–765.

Rizzolatti G, Camarda R, Fogassi L, Gentilucci M, Luppino G, Matelli M. Functional organization of inferior area 6 in the macaque monkey. *Exp Brain Res*. 1988:71:491–507.

Rizzolatti G, Fadiga L, Gallese V, Fogassi L. Premotor cortex and the recognition of motor actions. *Cogn Brain Res*. 1996:3:131–141.

Rizzolatti G, Cattaneo L, Fabbri-Destro M, Rozzi S. Cortical mechanisms underlying the organization of goal-directed actions and mirror neuron-based action understanding. *Physiol Rev*. 2014:94:655–706.

Russell B. *An inquiry into meaning and truth*. New York: Routledge; 1950

Schurz M, Radua J, Aichhorn M, Richlan F, Perner J. Fractionating theory of mind: a meta-analysis of functional brain imaging studies. *Neurosci Biobehav Rev*. 2014:42:9–34.

Searle JR. *Speech acts: an essay in the philosophy of language*. Cambridge, England: Cambridge University Press; 1969.

Searle JR. *Expression and meaning: studies in the theory of speech acts*. Cambrige, England: Cambridge University Press; 1985.

Searle JR, Vanderveken D. *Foundations of illocutionary logic*. Cambridge, England: Cambridge University Press; 1985.

Seed A, Byrne R. Animal tool-use. *Curr Biol*. 2010:20:R1032–R1039.

Seyfarth RM, Cheney DL, Marler P. Monkey responses to three different alarm calls: evidence of predator classification and semantic communication. *Science*. 1980:210:801–803.

Shibata M, Abe J-ı, Itoh H, Shimada K, Umeda S. Neural processing associated with comprehension of an indirect reply during a scenario reading task. *Neuropsychologia*. 2011:49: 3542–3550.

Smith SM. Fast robust automated brain extraction. *Hum Brain Mapp*. 2002:17:143–155.

Stelzer J, Chen Y, Turner R. Statistical inference and multiple testing correction in classification-based multi-voxel pattern analysis (MVPA): random permutations and cluster size control. *NeuroImage*. 2013:65:69–82.

Stout D, Chaminade T. Stone tools, language and the brain in human evolution. *Philos Trans R Soc B Biol Sci*. 2012:367:75–87.

Stout D, Toth N, Schick K, Chaminade T. Neural correlates of early stone age toolmaking: technology, language and cognition in human evolution. *Philos Trans R Soc B Biol Sci*. 2008:363: 1939–1949.

Thibault S, Py R, Gervasi AM, Salemme R, Koun E, Lövden M, Boulenger V, Roy AC, Brozzoli C. Tool use and language share syntactic processes and neural patterns in the basal ganglia. *Science*. 2021:374:eabe0874.

Thompson JA, Basista MJ, Wu W, Bertram R, Johnson F. Dual premotor contribution to songbird syllable variation. *J Neurosci*. 2011:31:322–330.

Tomasello R, Kim C, Dreyer FR, Grisoni L, Pulvermüller F. Neurophysiological evidence for rapid processing of verbal and gestural information in understanding communicative actions. *Sci Rep*. 2019:9:16285.

Tomasello R, Grisoni L, Boux I, Sammler D, Pulvermüller F. Instantaneous neural processing of communicative functions conveyed by speech prosody. *Cereb Cortex*. 2022:bhab522.

Tremblay P, Sato M, Small SL. TMS-induced modulation of action sentence priming in the ventral premotor cortex. *Neuropsychologia*. 2012:50:319–326.

Tylén K, Weed E, Wallentin M, Roepstorff A, Frith CD. Language as a tool for interacting minds. *Mind Lang*. 2010:25:3–29.

Urrutia M, Gennari SP, de Vega M. Counterfactuals in action: an fMRI study of counterfactual sentences describing physical effort. *Neuropsychologia*. 2012:50:3663–3672.

van Ackeren MJ, Casasanto D, Bekkering H, Hagoort P, Rueschemeyer S-A. Pragmatics in action: indirect requests engage theory of mind areas and the cortical motor network. *J Cogn Neurosci*. 2012:24:2237–2247.

Warren JE, Sauter DA, Eisner F, Wiland J, Dresner MA, Wise RJ, Rosen S, Scott SK. Positive emotions preferentially engage an auditory-motor "mirror" system. *J Neurosci*. 2006:26:13067–13075.

Watson Stuart K, Townsend Simon W, Schel Anne M, Wilke C, Wallace Emma K, Cheng L, West V, Slocombe KE. Vocal learning in the functionally referential food grunts of chimpanzees. *Curr Biol*. 2015:25:495–499.

Whorf BL. The relation of habitual thought and behavior to language. In: *Language, culture, and personality: essays in memory of edward sapir*. Menasha, Wisconsin: Sapir Memorial Publication Fund; 1941. pp. 75–93.

Willems RM, Labruna L, D'Esposito M, Ivry R, Casasanto D. A functional role for the motor system in language understanding: evidence from theta-burst transcranial magnetic stimulation. *Psychol Sci*. 2011:22:849–854.

Wilson SM, Saygin AP, Sereno MI, Iacoboni M. Listening to speech activates motor areas involved in speech production. *Nat Neurosci*. 2004:7:701–702.

Wittgenstein L. *Philosophical investigations*. Oxford: Blackwell; 1953

Xu J, Kemeny S, Park G, Frattali C, Braun A. Language in context: emergent features of word, sentence, and narrative comprehension. *NeuroImage*. 2005:25:1002–1015.

Zhang Y, Brady M, S. S. Segmentation of brain MR images through a hidden Markov random field model and the expectation-maximization algorithm. *IEEE Trans Med Imaging*. 2001:20:45–57.

Zwaan RA. Situation models, mental simulations, and abstract concepts in discourse comprehension. *Psychon Bull Rev*. 2016:23: 1028–1034.